



**EXPANSION AND SHRINKAGE STRAINS IN EXPANSIVE
REINFORCED CONCRETE STRUCTURES WITH THIN
SECTION**

BY

MS. SU HLAING MYINT

**A THESIS SUBMITTED IN PARTIAL FULFILMENT OF THE
REQUIREMENTS FOR THE DEGREE OF MASTER OF SCIENCE
(ENGINEERING AND TECHNOLOGY)
SIRINDHORN INTERNATIONAL INSTITUTE OF TECHNOLOGY
THAMMASAT UNIVERSITY
ACADEMIC YEAR 2019
COPYRIGHT OF THAMMASAT UNIVERSITY**

**EXPANSION AND SHRINKAGE STRAINS IN EXPANSIVE
REINFORCED CONCRETE STRUCTURES WITH THIN
SECTION**

BY

MS. SU HLAING MYINT

**A THESIS SUBMITTED IN PARTIAL FULFILMENT OF THE
REQUIREMENTS FOR THE DEGREE OF MASTER
OF SCIENCE (ENGINEERING AND TECHNOLOGY) SIRINDHORN
INTERNATIONAL INSTITUTE OF TECHNOLOGY
THAMMASAT UNIVERSITY
ACADEMIC YEAR 2019
COPYRIGHT OF THAMMASAT UNIVERSITY**

THAMMASAT UNIVERSITY
SIRINDHORN INTERNATIONAL INSTITUTE OF TECHNOLOGY

THESIS

BY

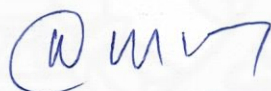
MS. SU HLAING MYINT

ENTITLED

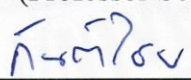
EXPANSION AND SHRINKAGE STRAINS IN EXPANSIVE REINFORCED
CONCRETE STRUCTURES WITH THIN SECTION

was approved as partial fulfillment of the requirements for
the degree of Master of Science (Engineering and Technology)

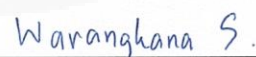
on June 26, 2020

Chairperson 


(Professor Somnuk Tangtermsirikul, D.Eng.)

Member and Advisor 

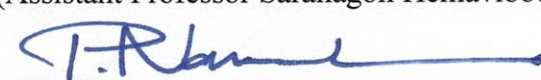
(Ganchai Tanapornraweekit, Ph.D.)

Member 

(Research Assistant Professor Warangkana Saengsoy, Ph.D.)

Member 

(Assistant Professor Saranagon Hemavibool, Ph.D.)

Director 

(Professor Pruettha Nanakorn, D.Eng.)

Thesis Title	EXPANSION AND SHRINKAGE STRAINS IN EXPANSIVE REINFORCED CONCRETE STRUCTURES WITH THIN SECTION
Author	Ms. Su Hlaing Myint
Degree	Master of Science (Engineering and Technology)
Faculty/University	Sirindhorn International Institute of Technology / Thammasat University
Thesis Advisor	Dr. Ganchai Tanapornraweekit
Academic Years	2019

ABSTRACT

Expansive cement or expansive additive is used to compensate the shrinkage strain in concrete under restrained condition. As the shrinkage cracks are commonly found in reinforced concrete structures having a large area with thin section, four types of reinforced concrete structures were selected to study their expansion and shrinkage strain under different restrained conditions. They are slab on beam and foundation, water tank wall, slab on grade, and industrial slab. Normal concrete and expansive concrete were used to observe different strain behaviour in these structures. Strain gauges and thermocouples were installed at different locations with different restraining degrees to monitor the strain and temperature profiles in each type of the monitored structure. The measured strains in this study are the total strains which include expansion and shrinkage strains under environmental effects and also external construction loading.

As there are limited amounts of study on expansion and shrinkage of reinforced concrete structures using expansive concrete, expansion and shrinkage strain profiles with different mix proportions under construction environment were studied. Moreover, the restrained expansion and shrinkage strains of the laboratory specimens are predicted from free strain using finite element analysis and verified with experimental data. The measurement results from selected reinforced concrete structures in construction sites

indicate that the locations which are exposed to the high temperature (sunlight) and low humidity environment, are more likely to show higher shrinkage strain. Therefore, moisture loss due to ambient temperature and humidity play a vital role in the formation of shrinkage strain. Additionally, external and internal degree of restraints according to their structural configuration are also important factors which can result in different expansion and shrinkage strains in each type of structure. In addition, the applied three-dimensional finite element (3D FE) method was useful to predict the expansion and shrinkage strains under restrained condition specimens as a good accuracy between 3D FE analysis and experimental data could be obtained. Moreover, the effectiveness of restrained tensile strain compensation in expansive concrete is presented through the strain measurement in construction sites, laboratory and the 3D FE modelling.

Keywords: Expansive additive, Reinforced concrete structures, Expansion and shrinkage strain, Restrained strains, 3D FE modelling

ACKNOWLEDGEMENT

First and foremost, the author would like to express her greatest gratitude to her advisor, Dr Ganchai Tanapornraweekit, for his comprehensive knowledge, guidance, and warm encouragement throughout the experimental works until the completion of this study. His expertise and persistence contributed to the improvement in this study and my knowledge.

The author wishes to give her sincere appreciation towards, the chairman of the examination committee, Prof. Dr Somnuk Tangtermsirikul, for guiding this research and providing opportunities to pursue her graduate study. Moreover, his constructive advice and suggestions in every aspect make this research interesting and provide contributions to the young researchers.

The author wants to thank her committee members, Dr Warangkana Saengsoy and Dr Saranagon Hemavibool, for their insightful comments, supports and guidance during this study. The author would like to acknowledge Sirindhorn International Institute of Technology, Thammasat University, for providing full scholarship during this study time. The author wishes to thank Siam Research and Innovation Co., Ltd and Denka Co., Ltd, and Centre of Excellence in Material Science, Construction and Maintenance Technology Project, Thammasat University for providing parts of a research fund for this study.

Thanks, are also extended to all the staff in student affairs and school secretaries who help me through this study time into convenient days without worrying about document works. My great appreciation is conveyed to all the technicians who helped me during my experiments with their patience and technical skill. Thanks to all students from the school of Civil Engineering and Technology who help me throughout my study time. Greatest thanks to Arosha Dabarera, Nguyen Bich Thuy, Phung Manh Cuong, Rachot Chatchawan, Krit Sukprasit, and Isuru Diaz who help me to accomplish my experimental works with their skillful experiences and knowledge. Special thanks to Hakas Prayuda, Suphawit Untimanon, Satish Paudel, and Rajendra Prasad Bohara for improving my research in every aspect. Thanks to my beloved friends: Su Su Nwal, Su Wutyi Hinin, Su Wai Hnin, Pyae Pyae Phyo, Tin Tin Khaing, Nasit Laosan, Hyunh

Tan Phong, Vu Duong, Bou Channa and Le Tran Tien Dat who understand and encourage me during study time.

Most of all, I would like to express my gratitude to my parents who support and strengthen me mentally and financially to achieve dreams and goals in my academic life.

Ms. Su Hlaing Myint



TABLE OF CONTENTS

	Page
ABSTRACT	(1)
ACKNOWLEDGEMENT	(3)
LIST OF TABLES	(8)
LIST OF FIGURES	(9)
CHAPTER 1 INTRODUCTION	
1.1 Background	1
1.2 Problem statements	3
1.3 Objectives of study	4
1.4 Scope of study	4
1.5 Significant of study	5
CHAPTER 2 LITERATURE REVIEW	6
2.1 Background	6
2.2 Expansive concrete tests in Laboratory	6
2.3 Study of non-expansive and expansive concrete in reinforced concrete structures	7
2.3.1 Study on shrinkage cracks in non-expansive concrete slabs	7
2.3.2 Study on shrinkage cracks in expansive concrete slabs	8
2.3.3 Study on shrinkage cracks in non-expansive and expansive concrete walls	10
2.3.4 Study on shrinkage cracks in non-expansive and expansive concrete pavements	11
CHAPTER 3 RESEARCH METHODOLOGY	14
3.1 General	14

3.2	Laboratory experiments	15
3.2.1	Mix proportions	17
3.2.2	Compressive strength (f_c')	19
3.2.3	Tensile stain capacity (TSC)	19
3.2.4	Free and restrained condition specimens in laboratory	20
3.3	Measurements in the construction site of SIIT new laboratory building	20
3.3.1	Measurements in slabs on beams and footings	21
3.3.2	Measurements in water tank walls	22
3.3.3	Measurements in slabs on ground (pavements)	24
3.4	Measurements in the construction site – industrial floor slabs	25
3.4.1	Measurements in normal concrete industrial floor slab (NC-Islab)	26
3.4.2	Measurements in expansive concrete industrial floor slab 1 (EA 1 Islab 1)	27
3.4.3	Measurements in expansive concrete industrial floor slab 2 (EA 2 Islab 2)	27
3.5	Method to predict restrained strain using finite element (FE) model	27
3.5.1	Finite element modelling	28
CHAPTER 4 RESULTS AND DISCUSSIONS		31
4.1	General	31
4.2	Laboratory experiment results	31
4.2.1	Compressive strength and tensile strain capacity tests results	31
4.2.2	Experimental results for laboratory specimens	33
4.3	Measurement results for SIIT new laboratory building	34
4.3.1	Measurement results for slabs on beams and footings	35
4.3.2	Measurement results for water tank walls	37
4.3.3	Measurement results for slab on grade (pavements)	39
4.4	Measurement results for industrial slabs (Islab)	46
4.4.1	Measurements results for NC-Islab	47
4.4.2	Measurements results for EA 1-Islab 1	51
4.4.3	Measurements results for EA 2-Islab 2	55

4.5 Prediction of restrained strain in expansive concrete specimens (prisms) by using Finite Element Analysis (FEA)	58
4.5.1 Applied loading from the experimental results	58
4.5.2 FE results of restrained specimens	59
CHAPTER 5 CONCLUSIONS AND RECOMMENDATIONS	65
5.1 Conclusions	65
5.2 Recommendations for future studies	66
REFERENCES	68
APPENDIX	
APPENDIX A	73
BIOGRAPHY	81

LIST OF TABLES

Tables	Page
3.1 Structure and related material types	14
3.2 Chemical compositions of cements and fly ash	16
3.3 Chemical compositions of expansive cements	17
3.4 Mix proportions for slabs on beams and footings	18
3.5 Mix proportions for water tank walls	18
3.6 Mix proportions for slabs on ground (pavements)	18
3.7 Mix proportions for industrial floor slabs	18
4.1 Compressive strength of concrete in all structural members	32
4.2 Tensile strain capacity of concrete in for all structural members	33
4.3 Modulus of rupture of concrete in for all structural members	33

LIST OF FIGURES

Figures	Page
1.1 Shrinkage and expansion of concrete under restrained conditions	3
1.2 Strain profiles under restrained condition	3
3.1 Framework of the studies	15
3.2 (a) Cylindrical moulds (b) compressive strength test	19
3.3 Prisms for tensile strain capacity test	19
3.4 Details of restrained specimen (all dimensions are in mm)	20
3.5 (a) Measurement locations for two slabs (b) Location 4 (c) Location 9	22
3.6 Plan view of the water tank	23
3.7 East wall and its measurement locations	23
3.8 North wall and its measurement locations	23
3.9 Plan view of pavements (All dimensions are in m)	24
3.10 Measurement locations of strain gauges and thermocouples (All dimensions are in m)	25
3.11 Plan view of industrial floor slabs	26
3.12 Measurement locations in NC-Islab	26
3.13 Measurement locations in EA 1-Islab 1	27
3.14 Measurement locations in EA 2-Islab 2	27
3.15 3D finite element model of the tested specimen	30
4.1 Expansion and shrinkage strains (a) free condition (b) restrained condition	34
4.2 Strain gauges installation through the depth of slab	36
4.3 Concrete temperature measured at location 4	36
4.4 Measured strain data from the longitudinal direction of EA-slab	36
4.5 (a) Horizontal steel strain at location 1 and 2 of the east wall (b) Vertical steel strain at location 3 and 4 of the east wall	38
4.6 (a) Horizontal steel strain at location 5,6, and 7 of the north wall (b) Vertical steel strain at location 5, 6, and 7 of the north wall	39
4.7 Concrete Temperature for Pavements	40
4.8 Locations of installed strain gauges in the section of pavement	41

4.9 Longitudinal strain in concrete at mid-depth and at steel layer (a) NC-Pave (b) EA 1-Pave 1 (c) EA 2-Pave 2 (d) EA 3-Pave 3	42
4.10 Layout of installed strain gauges at the centre of pavement	43
4.11 Longitudinal and transverse strain profiles at the slab centre (a)NC-Pave (b)EA 1-Pave 1 (c) EA 2-Pave 2 (d) EA 3-Pave 3	44
4.12 Strain gauges layout at centre and joint of pavement	45
4.13 Longitudinal strain in concrete at centre and joint (a) NC-Pave (b) EA 2- Pave 2 (c) EA 3-Pave 3	46
4.14 Concrete temperature in NC-Islab	47
4.15 Measured strains in short and long directions at location 1	48
4.16 Effect of perimeter beam to location 2	48
4.17 Measured strains in short and long directions at location 2 (a) at top existing steel (b) in concrete at mid-depth	49
4.18 Measured strains in short and long directions at location 3 (a) in steel (b) in concrete at mid-depth	50
4.19 Measured strains in short and long directions at location 4 (a) in steel at mid-depth (b) in concrete at mid-depth	51
4.20 Concrete temperature in EA 1-Islab 1	51
4.21 Effect of perimeter beam to location 7	52
4.22 Measured strain in short and long directions at location 7	53
4.23 Measured strains in short and long directions at location 8 (a) in steel at mid-depth (b) in concrete at mid-depth	54
4.24 Measured strain in short direction at location 9	54
4.25 Measured strain in short and long directions at location 10 (a) in steel at mid-depth (b) in concrete at mid-depth	56
4.26 Measured strains in short and long directions at location 11	57
4.27 Measured strain in short and long directions at location 12 (a) in steel (b) in concrete at mid-depth	58
4.28 Applied equivalent temperature curves	59
4.29 Illustration of expansive additive reaction in pore structures of concrete under restrained condition (a) partially hydration (b) fully hydration	60

4.30 Comparison of experimental and FE results (a) NC- Islab (b) EA 1- Islab 1 (c) EA 2- Islab 2	61
4.31 Maximum principal strain at mid-depth of the specimens (a) NC- Islab (b) EA 1- Islab 1 (c) EA 2- Islab 2	63
4.32 Maximum principal strain at end and middle part of specimens (a) NC- slab (b) EA 1- Islab 1 (c) EA 2- Islab 2	64



CHAPTER 1

INTRODUCTION

1.1 Background

Concrete is a mixture of cement, fine and coarse aggregates, water, and other chemical admixtures in appropriate ratios to get the desired strength. Conventional concrete has some weaknesses under restraint conditions. Volumetric change with restraint induces tensile stress inside the concrete. If the tensile stress reaches the tensile strength of the concrete, the concrete starts to crack which is a disadvantage for both appearance and the serviceability of the reinforced concrete structures. Stress initiation due to concrete expansion, shrinkage, or thermal effects is a complex mechanism for reinforced concrete structures in real environmental conditions (Neville & Brooks, 2010).

To reduce the shrinkage cracking, ACI 223R-10 introduced shrinkage compensating concrete or expansive cement to the construction industry since the mid-1960s. According to ACI 223R-10, there are four types of expansive cement used to mix with Portland cement i.e. type-K, type-M, type-S, and type-G. The first three types are ettringite formation type and Type-G is hydroxide platelet crystals formation type when mixed with Portland cement. There are other types of expansive cement or expansive additive, such as MgO based expansive concrete (Mo, Deng, Tang & Al-Tabbaa, 2014), high-performance expansive agents, etc.

The function of expansive concrete is that the volume of concrete is increased after setting time, and compressive stress is induced in concrete under restrained condition. There are mainly two types of restraints in reinforced concrete structures i.e., internal and external restraints. Coarse aggregate and reinforcements provide internal restraints. The amount of coarse aggregates and reinforcements are proportional to the level of expansion. Therefore, there is a proposed method to estimate the member expansion related to the percentage of reinforcement in ACI 223R-10. However, the prediction of degree of external restraints is more complicated than that of the internal restraints.

Other factors that can affect the level of expansion are binder content, water to binder ratio, chemical agent, curing condition, environmental condition (ambient temperature and relative humidity) and construction loading. The influences of these factors on the expansion level of expansive concrete have been found through conducting laboratory experiments (Lam, Sahamitmongkol & Tangtermsirikul, 2008; Lam et al., 2008; Nguyen, Sahamitmongkol, Lam, Tongaroonsri & Tangtermsirikul, 2010; Tongaroonsri & Tangtermsirikul, 2008). Even though the material scale behaviour of expansive concrete under different conditions is understood in the laboratory, it is still needed to understand its behaviour when using this material for structures under real conditions.

Shrinkage cracks could be found in reinforced concrete structures having large surface areas compared to its thickness, such as industrial floor slabs, slabs on ground, and water tank walls. These structures are most likely to have shrinkage cracks on their surfaces. For these types of structures, the internal restraints conditions cannot be reduced as the details of reinforcement layout are based on the structural design requirement. In addition, environmental loading cannot be controlled in the construction site. However, parts of external restraints from adjacent structural members and subgrade friction can be minimized for example by using expansion joints and providing plastic sheets between concrete body and subgrade.

To reduce shrinkage in these types of structures, expansive concrete is applied in this study to reduce shrinkage cracks. The mechanism of expansive concrete used in structural members is explained below. When the expansive concrete is used in a reinforced concrete structure that is restrained internally and externally, there is a formation of expansion strain inside the concrete. As a result, expansion strain due to expansive reaction can compensate the contraction strain resulted from the volume changes due to shrinkage under restraint conditions (see Figure 1.1 and Figure 1.2). Although the amount of expansion strain is directly proportional to the level of expansion under free condition, there is still a limited information to predict proper amount of an expansive additive to produce a sufficient expansion strain to compensate contraction strain under unknown degree of restraint resulted from both internal and external restraints and also from environmental effects in reinforced concrete structures.

To effectively compensate for the contraction strain caused by shrinkage, the proper amount of the expansive additive should be used.

The cracking on these types of structures has been carried out from various aspects especially by field investigations and numerical simulations. However, most of the previous researches were conducted for reinforced concrete structures using a non-expansive concrete type. Therefore, there have been needs to investigate the behaviour of structures using expansive concrete in the real field conditions.

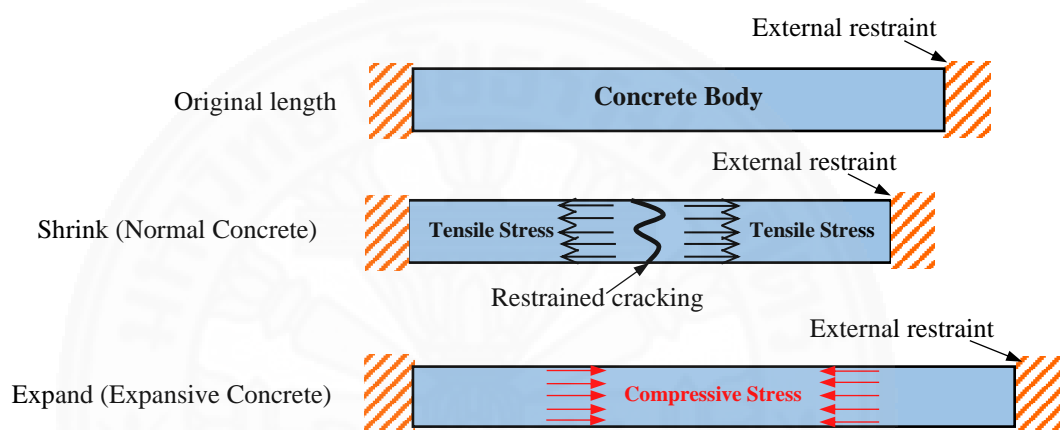


Figure 1.1 Shrinkage and expansion of concrete under restrained conditions

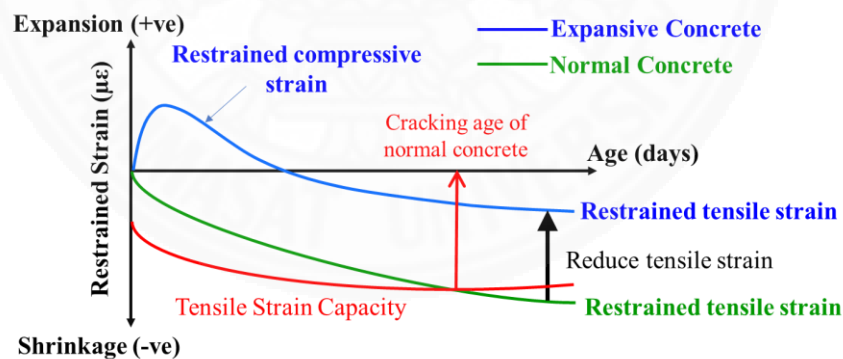


Figure 1.2 Strain profiles under restrained condition

1.2 Problem statements

Durability and sustainability of reinforced concrete structures are currently concerned for life cycles cost analysis of structures. Cracking is one source of deficiency in concrete structures which can reduce the durability of the structures. Shrinkage is one of the causes to form cracks. Therefore, the improvement of concrete

properties should be made to prevent shrinkage cracks. One of the preferable methods to reduce shrinkage cracking in reinforced concrete structure is the replacement of cement with a certain amount of expansive additive. Many researchers have studied the usage of expansive concrete and the behaviour of expansive additives with different testing methods which are briefly explained in chapter 2.

However, there is limited information on the evaluation of expansion/shrinkage of reinforced concrete structures using expansive concrete in a real application. Mostly, the structures having a large area with thin sections such as ground slabs, pavements, and reinforced concrete walls are more likely to have shrinkage cracks on their surfaces which can shorten the service life of those structures. In order to study the concrete cracks under restrained condition, the behaviour of restrained expansion/shrinkage strain profiles was monitored in field structures.

1.3 Objectives of study

To fulfill the gap of the research, field investigations were conducted in three different types of structures which were ground slabs, water tank walls and pavements of the newly constructed laboratory building of Sirindhorn International Institute of Technology, Thammasat University and also slabs in an industrial plant. Normal concrete and expansive concrete were used to cast those investigated structures. Restrained strains and temperature were monitored throughout the valid time in the construction sites. Therefore, the main objectives of this research are:

1. To evaluate expansion rates of EA concrete with different degrees of restraint
2. To study the strain profiles (both expansion and shrinkage) of the reinforced concrete structural elements such as slabs, water tank walls, and pavements under actual construction conditions and environments
3. To predict the restrained expansion and shrinkage strains of the laboratory specimens from the free expansion and shrinkage strains.

1.4 Scope of study

1. The measured strains in this study are the total strains (autogenous shrinkage, drying shrinkage and thermal strains).

2. The effects of dead load, environmental load and construction load are included in the measured strain profiles.
3. The measurement of strain profiles at the construction site is under the effect of actual environmental conditions where relative humidity and ambient temperature cannot be controlled.
4. Creep strain is not considered in this study.

1.5 Significance of study

In order to design the reinforced concrete structures using expansive concrete, it is important to know the level of expansion strain with their corresponding degree of restraints, type and content of expansive additive in the mix proportions. However, there is limited information for guideline of analysis and to design for reinforced concrete structures using expansive concrete. It is important to study the characteristics of reinforced concrete structures such as slabs, pavements, and water tank walls by using expansive concrete to support the application of expansive concrete.

CHAPTER 2

LITERATURE REVIEW

2.1 Background

The factors affecting shrinkage cracking of the reinforced concrete structures are material properties of concrete and steel, amount of reinforcement, boundary conditions to adjacent structural members, ambient temperature, and relative humidity of the construction environment. The level of expansion and shrinkage strain can be different according to their surrounding environment. Therefore, the performances of expansive concrete under controlled conditions were studied. The previous studies for expansive concrete in laboratory conditions are presented in Section 2.2.

Shrinkage cracking is one of the main problems for reinforced concrete structures having a thin section with large surface areas such as slabs, water tank walls, and pavements. Thus, expansive concrete has been popular for compensating shrinkage strain in these types of reinforced concrete structures. The overview of previous researches about non-expansive concrete and expansive concrete used in various types of slabs, walls, and pavements are provided in Section 2.3.

2.2 Expansive concrete tests in Laboratory

Durability tests for expansive concrete were conducted in the laboratory, and the test results showed that the ability of carbonation resistance could be improved in concrete using EA content lower than 20 kg/m^3 . However, the EA content should not be higher than 30 kg/m^3 since it will result in a lower carbonation resistance (Lam et al., 2008).

According to the previous studies from the laboratory experiments, the use of expansive additive with other cementitious materials such as fly ash or bottom ash or both types can increase the effectiveness in expansion strain and concrete compressive strength (Dung Tien Nguyen, 2010; Lam, Sahamitmongkol & Tangtermsirikul, 2008; Nguyen, Chatchawan, Saengsoy, Tangtermsirikul & Sugiyama, 2019; Pakorn Sutthiwaree, 2015). However, Nguyen et al. (2010) found that even though fly ash can increase expansion strain but a higher amount of fly ash can cause earlier crack initiation under restrained conditions.

The expansion and shrinkage strains are highly dependent on internal and external restraint conditions. Therefore, the influences of restrained conditions on expansive concrete become a part of research interest. Lam et al. (2008) and Dung Tien Nguyen (2010) reported that the higher the degree of restraint, the lower the net expansion values. Moreover, it also relies on the curing duration and curing methods.

One of the disadvantages of concrete is low tensile strength where crack can be easily initiated under restrained conditions. Nguyen et al. (2010) proposed the prediction of cracking age for both non-expansive concrete and expansive concrete with numerical equations and validated with the experimental results. The study showed that the actual cracking age is longer than the predicted cracking age. The difference between prediction and actual cracking age was concluded to be due to tensile creep, which can reduce the restrained shrinkage.

2.3 Study of non-expansive and expansive concrete in reinforced concrete structures

As cracks are detrimental to reinforced concrete structures in the long term, the causes of cracks become a concern. Shrinkage cracks are expected to form in structures having large areas with a thin section which is exposed to the high variation of ambient temperature and low humidity environment. It is important to study the shrinkage cracking on structures such as slabs, bridge decks, walls, pavements to maintain the serviceability and durability for a long service life of the structures. The previous studies on these types of structure with different approaches to investigate shrinkage cracks and the methods of reducing shrinkage cracks are presented below.

2.3.1 Study on shrinkage cracks in non-expansive concrete slabs

William, Shoukry and Riad (2005) studied the early-age cracking of bridge decks by measurement of strains in both concrete and reinforcement, cracks, and temperature of the bridge deck under environmental loading. It was found that drying shrinkage, traffic loading, and temperature variation through the depth and along the span length cause the tensile stress inside the bridge decks. These are the main causes of early age cracking in a bridge deck. Moreover, a high amount of restraints from formworks, abutments, and shear studs resulted high tensile stress in concrete as well.

Differential heat of hydration along the bridge deck due to different constituents of concrete mix was also a cause of premature crack.

Newell and Goggins (2017) monitored the strain profiles, temperature, and bending moment of the lattice girder slabs during the construction period. Vibrating wire strain gauges, thermistors, and electrical resistance strain gauges were installed in both precast plank and cast-in-situ slab. The restraint factors were calculated from the coefficient of thermal expansion of concrete under unrestrained (α_c) and restrained condition (α_r). α_c was assumed as $9 \mu\epsilon/^\circ\text{C}$ and α_r was calculated from the slope of strain and temperature of concrete under restrained condition. From the measurement, the highest concrete temperature was obtained from the mid-depth of the cast-in-situ slab. The prediction of measured strain using Eurocode 2 (BSI, 2004) was in a good agreement with non-thermal measured strain. The value of creep, concrete properties and relative humidity were assumed in the calculation.

Kanciruk (2018) investigated temperature, strain, material aging and service load effects on the slab of the aircraft hangar. After a 5-year measurement was done, the recorded strains were derived based on temperature changes, and impact load from the airplane. These are the reasons which can form micro scratches on floor slabs.

Newell and Goggins (2018) studied thermal behaviour of the hybrid precast concrete floor under the construction environment through structural health monitoring. Strain inside the precast and cast in situ portions were monitored and these measured strains were a combination of shrinkage, flexural and creep strains. The measurement results were compared with 1-dimensional finite element analysis. Parameters considered in the numerical model are conduction, convection, solar radiation, and thermal irradiation properties. The implemented one-dimensional numerical model was used to predict the thermal variations in the slab. The authors also suggested that a good care should be taken to design the slabs exposed to high solar radiation in which the solar radiation can affect high-temperature variation through the slab depth which consequently changes the curvature of the slab.

2.3.2 Study on shrinkage cracks in expansive concrete slabs

Michael D. Brown and John (2007) proposed to reduce drying shrinkage cracks on bridge decks by using various materials, i.e. high-performance concrete (HPC), high

volume fly ash concrete (HVFC), shrinkage compensating concrete (CSA), shrinkage reducing admixture (SRA) and fibres. Laboratory specimens and prototype bridge decks were used to study the effects of those different materials. The ring test results of control mix and HPC mix showed that cracks were observed at 20 days and 19 days, respectively. It is also found that the prototype bridge decks using control mix and HPC mix showed mid-transverse cracking and the other prototype bridge decks using HVFC, CSA, SRA and fibres did not show any crack. Therefore, the authors using HVFC, CSA, SRA and fibres concrete to resist early-age cracks on bridge decks due to drying shrinkage.

Field measurements were conducted in the post-tensioned concrete slab which was cast with shrinkage compensating concrete. Vibrating wire strain gauges and thermistors were mainly installed at the base of the column and the middle of the slab. After two years of measurement, it was found that the use of shrinkage compensating concrete in the post-tensioned slab could reduce nearly 50 per cent of shrinkage strain compared to the predicted shrinkage strain using normal concrete. The fluctuation of the measured strains were resulted from the daily temperature changes, and the surrounded construction activities near the measured locations (Richardson, Schiller & Mike, 2010).

Long term investigation of dam foundation which used a new shrinkage reducing admixture, MgO expansive additive, were studied for ten years of service condition. According to the measurement, MgO expansion agent is good for maintaining the volumetric deformation of the mass concrete foundation of the dam during low ambient temperature. Due to this contribution of MgO expansive concrete, the cost and time of the project can be shortened (Chen, Tang & Zhao, 2011).

Liu, Shen, Hou, Arulrajah and Horpibulsuk (2016) studied underground structures (floor and wall) which were improved by using expansive concrete. Strain measurements were conducted in field structures and also laboratory specimens. Due to proper curing for laboratory specimens, the maximum restrained expansion strains of specimens in the laboratory were higher than those of specimens under field curing condition. Furthermore, proper curing conditions are important for expansive concrete. The transportation time between the mixing plant and construction site should be minimized in order to maintain the expansion rate in the field structure. The study found

that the field structures can maintain longer expansion strain due to intensive restrained condition from the structure under long-term.

Ishida, Pen, Tanaka, Kashimura and Iwaki (2018) performed a computational analysis that can verify and validate the shrinkage strain and temperature profile results with measurement data from small scale specimens to the actual structure. There were deviations of strain results between computational models and the measurements which were likely to come from the influence of curing and ambient condition such as rainfall and wind. To be concluded, the overall verification results between numerical analysis and measured results of multiscale models showed a good agreement under an acceptable range.

2.3.3 Study on shrinkage cracks in non-expansive and expansive concrete walls

Carlson and Reading (1988) studied the effects of base restraint to the behaviour of four different length (L) to height (H) ratios ($L/H=1$, $L/H=2$, $L/H=4$, and $L/H=12/7$). The study found that the maximum tensile stress was observed in the horizontal direction near the foundation in $L/H=2$. In long wall structure (e.g. $L/H=4$), high tensile stress can be observed along the wall height. Tensile stress at the centre of the wall showed 40% of maximum tensile stress at the base of the wall. Therefore, providing slip joint, roller foundation, joints, and the proper amount of reinforcement can reduce the tensile stress and cracks due to base restraint.

Rawil and Kheder (1990) studied for the factors affecting cracking of the concrete walls such as length by height (L/H) ratios, base restraint, volume changes, drying shrinkage and thermal shrinkage. As the degree of restraint was varied along the wall height, the authors suggested reducing the cracks based on their studies by (1) reduce the L/H ratio (2) the distribution of reinforcement is required to be varied according to the levels of base restraint.

Kheder (1997) conducted 37 full-scale walls and 8 experimental walls. Six different length to height (L/H) ratios were tested in the laboratory to know the effect of reinforcement along the wall. After conducting the experiments, the relationship between L/H ratio and the amount of reinforcement to control the crack width was found. The amount of reinforcement can be varied along with the height of the wall with respect to their degree of restraint. The authors suggested that by providing a

smaller L/H ratio to reduce the degree of restraint and to reduce the amount of reinforcement.

To investigate the cracks on the wall, Attiyah, Gesund, Mohammed, Rasool and Rasool (2014) proposed a 3-dimensional finite element (3D FE) model using ANSYS. Wall structures were modelled with solid elements for concrete and beam elements for reinforcing bar. The measured shrinkage strain was converted into temperature strain and applied to the 3D FE model. The prediction of crack width showed a good agreement with the measured results.

Li, Tian, Zhao, Lu and Liu (2018) used MgO expansive agents with three types of reactivity rates for the tested specimens, which were walls and mass concrete structures. The study found that the expansion strains were highly dependent on the ambient temperature. Under high cooling temperature, the low reactivity MgO expansive concrete showed higher expansion strain than high reactivity one. However, high expansion strains were resulted from MgO expansive agents with high reactivity under low cooling rates with high temperature such as mass concrete structure.

Yu, Deng, Mo, Liu and Jiang (2019) studied about the reaction mechanism and expansion strain of the lightly burn MgO expansive agent. MgO expansive agent with higher hydration reactivity led to brucite formation which could fill the pores or micro voids and made the concrete denser. MgO with higher hydration reactivity led to a lower expansion rate.

2.3.4 Study on shrinkage cracks in non-expansive and expansive concrete pavements

Rebibou, Dux and Nooru-Mohamed (2003) studied about concrete shrinkage behaviour of laboratory specimens and the pavements. They installed the embedded strain gauges at different depths of the pavement to measure about shrinkage strain and temperature. From the laboratory experiment, the study found that large differential strain values through the depth were observed in uncured specimens. The early age cracking on pavements was due to differential strains through the depth which was resulted from hydration, suction, and restraint.

Seongcheol and Moon (2010) studied thermal and drying shrinkage strains using impervious and pervious cylinders under field conditions. Vibrating wire strain

gauges, temperature and relative humidity (RH) sensors were installed in post-tensioned pavement and thin slab to measure the relation of drying shrinkage with the temperature and RH inside the slab. From these measurements, the moisture gradient through the cross-section could be observed in both specimens and the thin slab. Moreover, the authors found that the coefficient of thermal expansion of concrete is varied along with time and curing conditions.

Asbahan and Vandebossche (2011) studied the curvature of the pavement through temperature and moisture profiles. This study showed that curling and warping of pavement were resulted from the temperature difference between the ambient and concrete temperature. The thicker the pavement, the higher in temperature difference in depths, which can encourage the higher upward and downward curl on the pavement. Restrained pavement showed much more effective in the reduction of drying shrinkage and reduce the curvature of the pavement due to moisture gradient than unrestrained pavement.

The early age cracking and volume stability of the pavement were improved by using MgO expansive agent with hybrid fibre. The use of MgO expansion agents with hybrid fibres can compensate early age shrinkage, although the higher amount of hybrid fibres (such as 80 kg/m³) reduced the expansion strain. Furthermore, the use of hybrid fibres reduced macrocracking and microcracking inside the cement paste, which could control the volume stability of the concrete (Huang, Deng, Mo & Wang, 2013).

Adriano, Sergio, Maurizio, Massimo and Giovanni (2015) studied a jointless floor with experiment and numerical analysis. Two types of cementitious materials (calcium sulpho-aluminate (CSA) cement and ordinary Portland cement) were used to observe the curvature of the pavement. CSA encourages the volume stabilization of the pavement in both longitudinal and transverse directions by producing compressive stress during the curing period. This leads to a reduction in curling at the boundaries of the pavement due to the linear shrinkage gradient through the thickness. By performing numerical analysis, the different behaviour between shrinkage compensating concrete pavement and ordinary Portland concrete pavement were significantly observed. Compressive stresses in concrete were observed in shrinkage compensating concrete due to restrained from reinforcement and base friction.

Chris Ramseyer and Seth (2016) applied Type-K shrinkage compensating concrete in water tank walls, water tank slabs, and slabs-on-ground under restrained and unrestrained conditions. The overall results from measurements of total strain from walls, base slabs, and slabs-on-grade were observed. The results showed that type-K shrinkage compensating concrete were effective. The authors concluded that the lowest surface area with high volume specimens showed higher expansion as moisture could be stored longer inside the specimen and small surface area for moisture loss.

Huang et al. (2019) used MgO expansive agents in the jointed concrete pavement to reduce shrinkage cracking under severe environmental conditions. MgO expansion agent was applied in reinforced concrete pavements at the airport with mainly two sizes: 4 m x 4 m and 8 m x 4 m under high daily temperature variation environment. The results showed that the widths of the transverse cracks in pavements could be effectively reduced by using MgO expansive agent and by providing a proper amount of reinforcement.

CHAPTER 3

RESEARCH METHODOLOGY

3.1 General

This chapter mainly focuses on understanding the behaviour of expansion and shrinkage strain in reinforced concrete structures with different mix proportions under the construction site environment. Four different types of structures: slabs on beam and footings, water tank walls, slabs on ground (pavement), and industrial floor slabs were studied. A brief explanation of types of structures related to their concrete type used is presented in Table 3.1. Three different chemical compositions of expansive additive were used. S-3P and S-2P were from the Siam Research and Innovation Co., Ltd and D was from DENKA Co., Ltd. The methodology for this study is divided into two main parts. Firstly, experiments were conducted in the laboratory for compressive strength, tensile strain capacity for different concrete mix proportions which were used in verifying strain measurement data of structural members in a real construction site. Secondly, strain measurement in the real construction sites was conducted in order to investigate the expansion and shrinkage strains in slabs on beams and footings, water tank walls, and slabs on ground. Moreover, the restrained expansion and shrinkage strain profiles of the specimens were predicted with finite element analysis. The framework of this study is illustrated in Figure 3.1.

Table 3.1 Structure and related material types

No.	Structure	Type of Concrete	Brand of EA	Symbol
1.	Slabs on beams and footings	Normal concrete	-	NC-slab
		Expansive Concrete	S-3P	EA-slab
2.	Water tank walls	Expansive Concrete	S-3P	EA-WT
3.	Slabs on ground (pavements)	Normal concrete	-	NC-pave
		Expansive Concrete 1	S-3P	EA 1-pave 1
		Expansive Concrete 2	D	EA 2-pave 2
		Expansive Concrete 3	S-2P	EA 3-pave 3
4.	Industrial slabs	Normal concrete	-	NC-Islab
		Expansive Concrete 1	S-2P	EA 1- Islab 1
		Expansive Concrete 2	D	EA 2- Islab 2

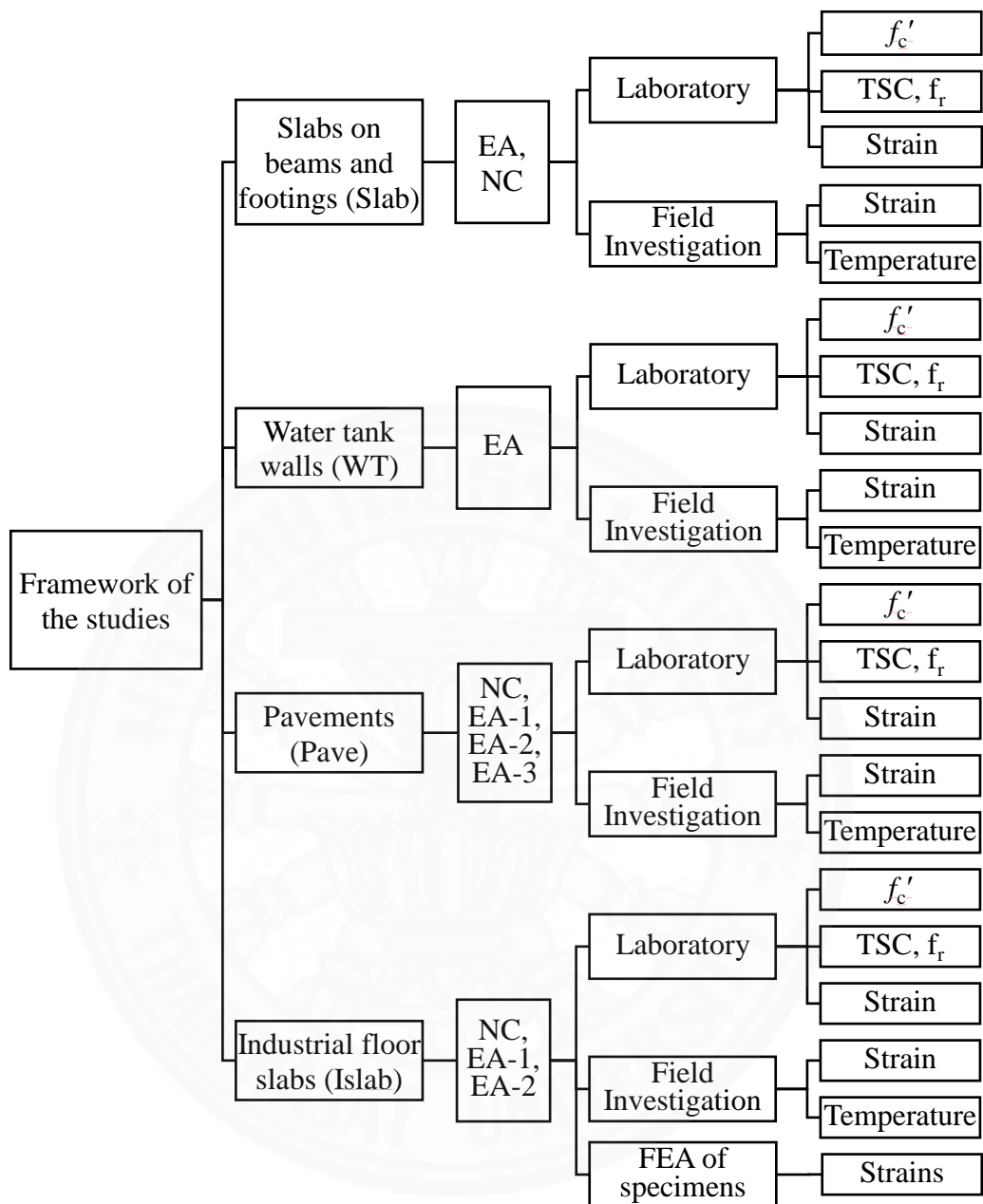


Figure 3.1 Framework of the studies

3.2 Laboratory experiments

Ten mix proportions were used for casting four different types of structural members. These mix proportions were obtained from a ready-mixed concrete plant of CPAC (The concrete products and aggregate Co., Ltd). The definitions of materials composed in mix proportions are explained below. The chemical compositions of cement, fly ash, and expansive additive are presented in Table 3.2 and,

Table 3.3 respectively.

1. Cement – Type I cement (ordinary Portland cement) and hydraulic cement (cement with limestone powder) were used for all mix proportions. These cements are the products of Siam Cement Co., Ltd.
2. Fly ash – Mae Moh fly ash was used in all the mix proportions. The fly ash was obtained from the Mae Moh electrical power plant in the northern part of Thailand.
3. Expansive additives –Two commercial brands, one from Siam Research and Innovation Co., Ltd (S-3P and S-2P) and another from Denka Co., Ltd (D) were used in this study. S-3P and SP-2P are the expansive additive (the combination of ettringite and Ca(OH)₂ formation type) with different chemical compositions and D is the expansive additive of ettringite formation type (see
4. Table 3.3).
5. Aggregates – River sand was used as the fine aggregate. Two types of coarse aggregate with a maximum size of 19 mm, conventional coarse aggregate and recycled concrete aggregate, were used in all the mix proportions.
6. Chemical admixtures – Type D and type F chemical admixtures were added to the mix proportions. Type D is a water-reducing and set-retarding admixture and type F is a high range water-reducing admixture.

Table 3.2 Chemical compositions of cement and fly ash

Chemical/mineral compositions	Cement		Fly ash (Mae Moh)
	Type I	Hydraulic cement	
SiO ₂	19.6	18.9	36.18
Al ₂ O ₃	5.4	5.1	20.21
Fe ₂ O ₃	3.2	3.1	13.89
CaO	62.3	63.7	18.74
MgO	1.4	1.4	2.69
K ₂ O	0.6	0.6	2.29
SO ₃	2.9	2.7	3.74
Na ₂ O	0.2	0.2	1.14
C ₃ S	55.6	68.8	-
C ₂ S	14.3	2.3	-
C ₃ A	8.7	8.3	-
C ₄ AF	9.9	9.6	-

Table 3.3 Chemical compositions of expansive additives

Chemical compositions	Expansive additive (S-3P)	Expansive additive (S-2P)	Expansive additive (D)
SiO ₂	2.45	6.4	1.93
Al ₂ O ₃	5.21	1.74	5.03
Fe ₂ O ₃	0.19	1.09	1.22
CaO	61.85	74.59	69.47
MgO	0.6	0.93	1.04
K ₂ O	-	0.12	0.05
SO ₃	25.8	10.69	17.7
Na ₂ O	-	-	<0.01
TiO ₂	-	0.09	0.05
P ₂ O ₅	-	0.08	0.09
MnO	-	0.03	0.03
SrO	0.11	0.04	0.02
ZnO	-	0.01	0.01
CuO	-	-	0.02
Free lime	-	-	46.98
LOI	3.7	4.11	3.3

3.2.1 Mix proportions

Mix proportions were different in each considered structural members. For each mix proportion, the basic material properties such as compressive strength, tensile strain capacity and modulus of rupture were tested in the laboratory. Normal concrete (NC) and various type of expansive concrete (EA) were mainly used for each studied reinforced concrete structural member. Mix proportions for slabs on beams and footings (Slab), water tanks walls (WT), pavements (Pave), and industrial floor slabs (Islab) were presented in Table 3.4, Table 3.5, Table 3.6, and Table 3.7, respectively.

Table 3.4 Mix proportions for slabs on beams and footings

Name	Cementitious Materials (kg/ m ³)			Water (l/m ³)	Aggregate (kg/ m ³)		Admixture (ml/ m ³)	
	Cement Type 1	Fly Ash	Expansive Additive		Fine	Coarse	Type D	Type F
NC-slab	252	64	-	190	880	1040	1256	500
EA-slab	222	64	30	190	880	1040	1175	1500

Table 3.5 Mix proportions for water tank walls

Name	Cementitious Materials (kg/ m ³)			Water (l/m ³)	Aggregate (kg/ m ³)		Admixture (ml/ m ³)	
	Cement Type 1	Fly Ash	Expansive Additive		Fine	Coarse	Type D	Type F
EA-WT	179	171	30	175	820	1070	505	1600

Table 3.6 Mix proportions for slabs on ground (pavements)

Name	Cementitious Materials (kg/ m ³)			Water (l/m ³)	Aggregate (kg/ m ³)		Admixture (ml/ m ³)	
	Hydraulic Cement	Fly Ash	Expansive Additive		Fine	Coarse	Type D	Type F
NC-Pave	270	30	-	190	840	1100	1090	500
EA 1-Pave 1	245	30	25	190	840	1100	1090	1100
EA 2-Pave 2	250	30	20	190	840	1100	1090	900
EA 3-Pave 3	245	30	25	190	840	1100	1090	1200

Table 3.7 Mix proportions for industrial floor slabs

Name	Cementitious Materials (kg/m ³)			Water (l/m ³)	Aggregate (kg/m ³)		Admixture (ml/m ³)	
	Cement Type 1	Fly Ash	Expansive Additive		Fine	Coarse	Type D	Type F
NC-Islab	226	54	-	185	930	1040	791	1600
EA 1-Islab 1	201	54	25	185	930	1040	800	1700
EA 2- Islab 2	206	54	20	185	930	1040	791	1600

3.2.2 Compressive strength (f_c')

The compressive strength test procedure is according to the ASTM C39/C39M-08. Cylindrical specimens with 100 mm in diameter and 200 mm in height were used to test compressive strength each mix proportion. Three specimens were tested for each type of concrete at the ages of 1 day, 3 days, 7 days, and 28 days. The compressive strength specimens are shown in Figure 3.2. The specimens demoulded one day after casting were placed in the open space in the laboratory in order to imitate the curing condition of the structural members in the real construction site.



Figure 3.2 (a) Cylindrical moulds (b) compressive strength test

3.2.3 Tensile strain capacity (TSC)

Tensile strain capacity tests were conducted in order to determine the cracking strain of the concrete. The test procedure followed ASTM C78/C78M-08. The prism size was 100 mm \times 100 mm \times 350 mm. Strain gauges were glued at the tension face of the prism to measure the tensile strain of the concrete (see Figure 3.3). Testing age of 1 day, 3 days, 7 days, and 28 days were selected, and two prisms were tested for each testing age. The curing method was the same as that used for compressive strength specimens.



Figure 3.3 Prisms for tensile strain capacity test

3.2.4 Free and restrained condition specimens in laboratory

Laboratory specimens were cast using the same batch of concrete used for casting slab in the construction site. Strain profiles were measured in free and restrained conditions by following ASTM C157/C157M-08 and ASTM C878/C878M-08, respectively. Restrained expansion/shrinkage concrete prisms conformed to ASTM C878 with some slight modifications in which the details will be given later. Three specimens were collected for each mix proportions to obtain the average strain value.

For free condition test, the specimen size is 75 mm × 75 mm × 285 mm according to ASTM C157. The specimens were cast at the concrete batching plant. The specimens were left at the batching plant for one day to minimize the disturbance, which could affect the unmaturing concrete specimens. Then, the measurements were started after 1-day (at the age of approximately 1 day) when the specimens were taken back to the university laboratory. Both free and restrained conditions specimens were placed in the controlled room with 28 °C temperature and 70% relative humidity.

Restrained condition specimens were tested by following ASTM C878 standard with some slight modifications. The specimen size is 100 mm × 100 mm × 350 mm, two steel endplates were fixed at both ends, and a 12 mm diameter deformed bar was placed at the mid-section of the specimen. The length change measurement method for restrained specimens was modified from the use of a length comparator to an electrical resistance strain gauge which was attached at the mid-length of the reinforcing bar (see Figure 3.4). Measurement was started immediately after the concrete was cast in the mould (day 0).

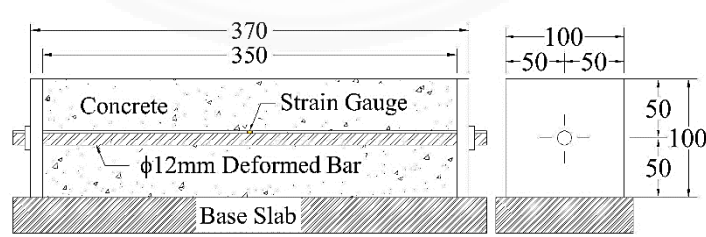


Figure 3.4 Details of restrained specimen (all dimensions are in mm)

3.3 Measurements in the construction site of SIIT new laboratory building

Three different structural elements were chosen for measuring the expansion and shrinkage strains at different locations with different conditions of restraint. They

are two slabs on beam and footings, two water tank walls, and four pavements. Three following subsections demonstrate the strain gauges and thermocouple installation in each structural member in different locations. The details plan and sections of the tested structures, slabs, walls, pavements, and industrial floor slabs, are presented in Appendix A.

Because of the fluctuation of measured strain during the plastic stage of concrete, the plotted measured strains were intended to be initialized at the final setting time of the concrete. It should be noted that the final setting times of concrete at different locations of the structures are different as the concrete casting cannot be quickly finished for the large area of concrete casting, and the concrete transportation time from the ready-mixed concrete plant to the construction site could not be controlled. Therefore, the final setting time is assumed to be about 8 hours after finished casting in this study.

In slabs on beams and footings and water tank walls, the measured strains showed large fluctuations before final setting time. Therefore, the measured strain data for these two structures are initialized after setting time to compare the strains at different measured directions. It is noted that initializing at final setting time is reasonable as the restrained strain would be initiated after the concrete hardened. For the slabs on ground (pavements), there was a technical problem in transferring the measured strain data to the data logger at the first 7 days. Thus, the initialized time was taken as at the time of finished casting for the slab on ground (pavements). It is noted that the implementation of different initialized time of the strain plots does not have any problem because there was no intention to compare the strain across structure types and also there was no intention to conduct quantitative analysis but only comparative analysis of the strains at the same location within the same structure.

3.3.1 Measurements in slabs on beams and footings

Locations of strain and temperature measurement were selected with respect to their different boundary conditions such as adjacent structural elements, supporting members as well as the reinforcement ratio of the member. Strain gauges were arranged in both longitudinal and transverse directions of the slab in order to measure expansion and shrinkage strain profiles in those two directions. Strain measurements were done

for both concrete and steel. Strain gauges for steel were installed at the top and bottom reinforcement of the slab, and concrete strain gauges were installed at the mid-depth of the slab. A thermocouple was installed at the mid-depth of the slab to record the concrete temperature measuring point.

Measurement locations in expansive concrete and normal concrete slabs were carefully selected to have as much as possible the same reinforcement and external restraint conditions. The selected measurement locations in both slabs are shown in Figure 3.5 (a). The strain gauges arrangements, for example, of location 4 in the expansive concrete slab and location 9 in the normal concrete slab are shown in Figure 3.5 (b) and (c), respectively. The detail drawing of the slab is shown in Appendix A.

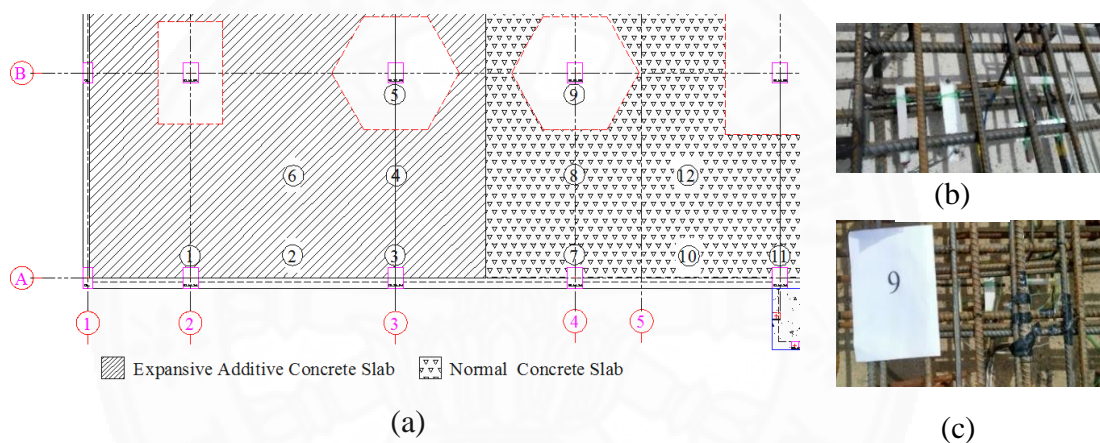


Figure 3.5 (a) Measurement locations for two slabs (b) Location 4 (c) Location 9

3.3.2 Measurements in water tank walls

Shrinkage cracking causes detrimental effects on the water tank wall. Roof water tank walls are exposed to a variation of ambient temperature and humidity during day and night times. Therefore, expansive concrete was introduced to reduce shrinkage cracking for this type of structure. Two walls were selected to analyse the strain profiles under restrained conditions from the adjacent structural members. The strain measurement on the east wall was performed to study the effect of the sunlight. Moreover, the strain in the north wall of the water tank was also monitored to study the expansion and shrinkage strains under less sunlight exposure. The measured locations were selected to observe strain profiles (expansion and shrinkage strains) under different restrained degrees due to the amount of reinforcement, base slab, top slab, and adjacent walls. Four locations in the east wall and three locations in the north wall were

selected for strain measurements. In each wall, strain gauges were attached to the horizontal and vertical directions rebars in both outer and inner faces of the wall.

Strain gauges were installed at both outer and inner faces of the wall to investigate the effects of moisture loss on expansion and shrinkage strains of the wall, The plan view of the water tank and the selected wall panels are illustrated in Figure 3.6. Section of the water tank is illustrated in Appendix A. The selected locations of strain measurement in the east, and north walls are shown in Figure 3.7 and Figure 3.8, respectively.

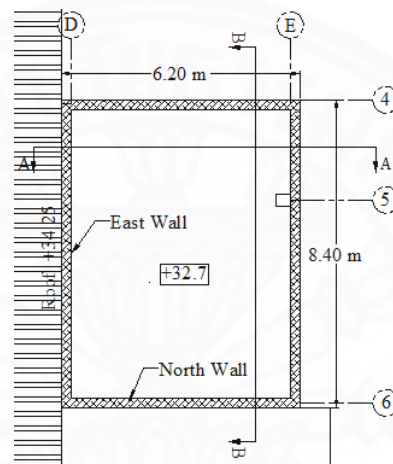


Figure 3.6 Plan view of the water tank

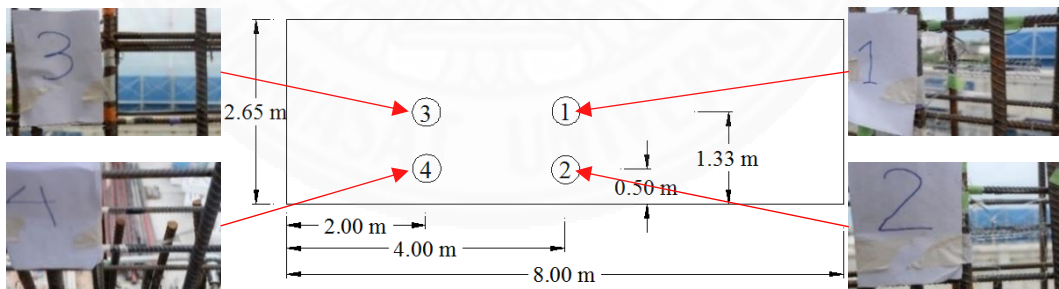


Figure 3.7 East wall and its measurement locations

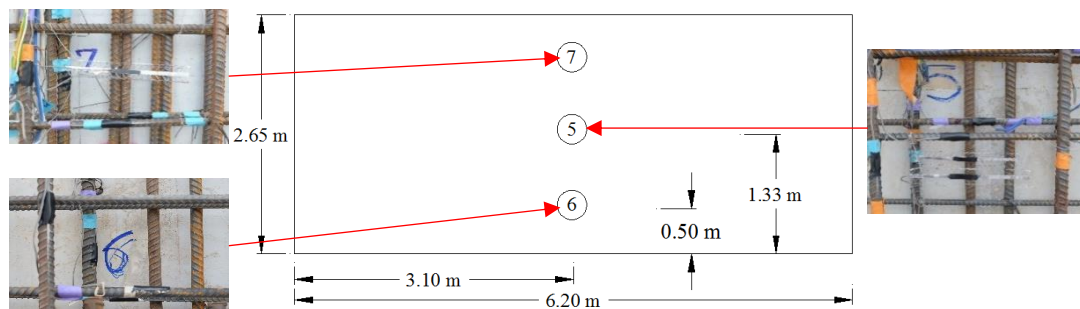


Figure 3.8 North wall and its measurement locations

3.3.3 Measurements in slabs on ground (pavements)

Four different types of concrete, normal concrete (NC-Pave) and three different expansive concrete (EA 1-Pave 1, EA 2-Pave 2 and EA 3-Pave 3), were used to cast four pavements. Two measurement locations, at the centre and near the expansion joint, were selected to investigate the strain and temperature profiles for each type of pavement.

The dimensions of the pavements are $12.8 \text{ m} \times 4.6 \text{ m} \times 0.15 \text{ m}$. Wire mesh with 6-mm deformed bars having 200-mm spacing were provided in longitudinal and transverse directions of the pavement at a depth of 35 mm from the top surface. Deformed bars with 25 mm diameter having 300-mm spacing were provided at the expansion joint. The pavements were laid over 150 mm thickness of the crush rock base.

As the strain in the pavement was affected not only by the base restraint but also the environmental effects, strain gauges were installed at different depths, e.g. at the layer of wire mesh reinforcement (35 mm from the surface) and at the mid-depth (75 mm from the surface) for all the pavements. The purpose of measurements were (i) to observe the effects of moisture loss through the depth of the pavement (ii) to investigate the effects of base friction in both longitudinal and transverse directions. The overall plan views of the pavements and the locations of installed strain gauges for each pavement are shown in Figure 3.9 and Figure 3.10, respectively. The detail plans of pavement are illustrated in Appendix A.

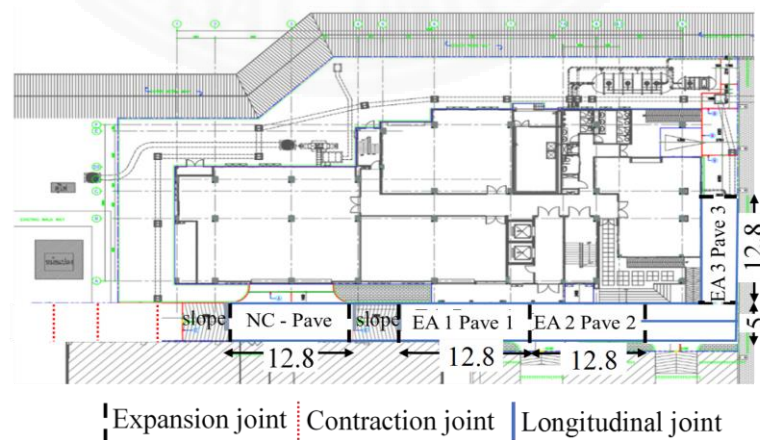


Figure 3.9 Plan view of pavements (All dimensions are in m)

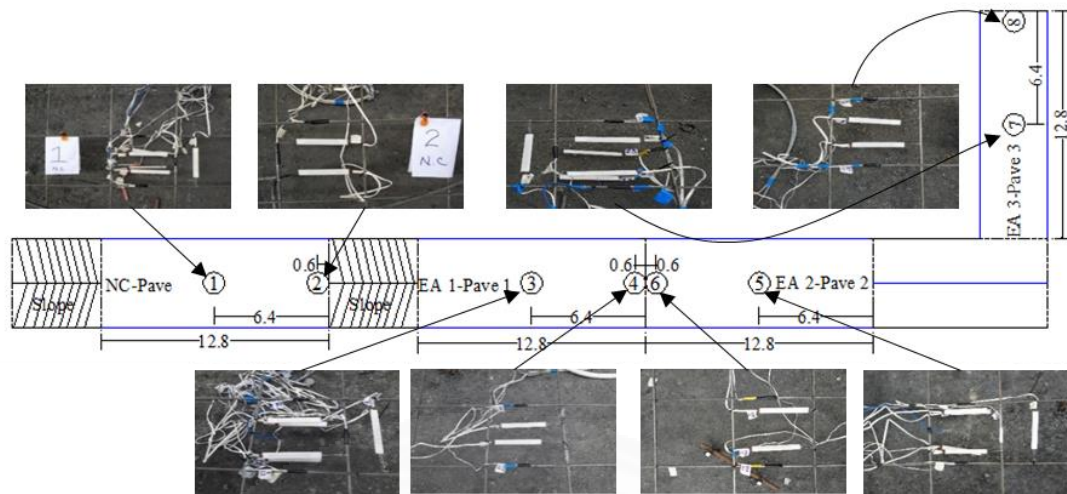


Figure 3.10 Measurement locations of strain gauges and thermocouples (All dimensions are in m)

3.4 Measurements in the construction site – industrial floor slabs

The ground slabs of one industrial building were selected to study the strains with different degrees of restraint in each slab resulted from base friction in long and short directions, adjacent structural members, and foundation. Three slabs were selected among a total of ten in the whole area of the ground floor of the building (see Figure 3.11). Three different types of concrete were used to cast the ground slab (i.e. one type of normal concrete (NC-Islab), two different commercial brands of expansive additive concrete (EA 1-Islab 1 and EA 2-Islab 2)). The detail plans and sections of industrial slabs are shown in Appendix A. It is noted that the initial time (Time= 0 day) of the measured strains was set at after casting time is finished as there is no large fluctuation in the recorded strains in concrete during casting time and final setting time of the concrete.

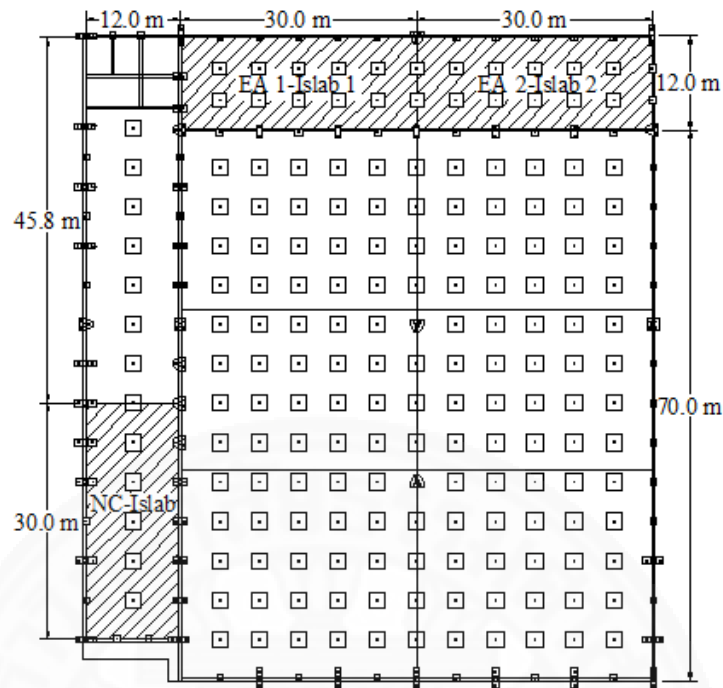


Figure 3.11 Plan view of industrial floor slabs

3.4.1 Measurements in normal concrete industrial floor slab (NC-Islab)

Four different types of restrained conditions were selected to install the strain gauges and thermocouples in NC-Islab. Measurement locations are shown in Figure 3.12. Location 1 was expected to be restrained by the adjacent two footings while the location 2 and location 3 were restrained by a beam in one direction, and location 4 was restrained by beams in two directions.

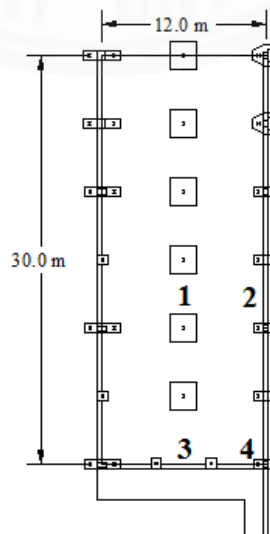


Figure 3.12 Measurement locations in NC-Islab

3.4.2 Measurements in expansive concrete industrial floor slab 1 (EA 1-Islab 1)

Three locations were chosen to install the strain gauges and thermocouples in EA 1-Islab 1 (see Figure 3.13). In this slab, location 7 was at a distance 70 cm from the ground beam, location 8 was in the middle between two footings, and location 9 was between the perimeter beam and footings.

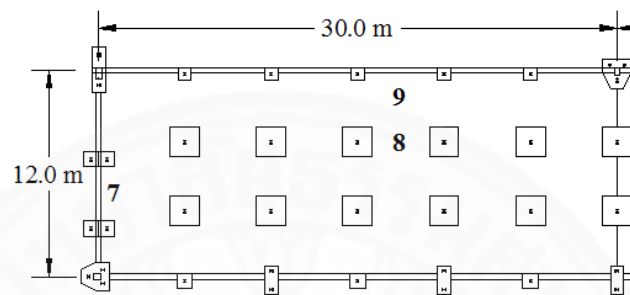


Figure 3.13 Measurement locations in EA 1-Islab 1

3.4.3 Measurements in expansive concrete industrial slab 2 (EA 2-Islab 2)

Measurement locations in EA 2-Islab 2 were selected to resemble the measured locations used in EA 1-Islab 1. Therefore, location 10 was in the middle of the perimeter beam and footings, location 11 was placed in the middle of two footings, and location 12 was at 70 cm away from the adjacent perimeter beam. Locations for EA 2-Islab 2 are illustrated in Figure 3.14.

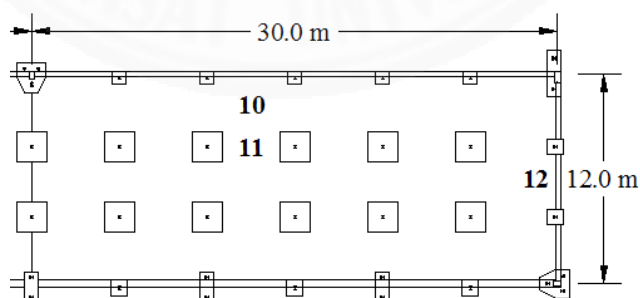


Figure 3.14 Measurement locations in EA 2-Islab 2

3.5 Method to predict restrained strain using finite element (FE) model

Free condition and restrained condition specimens were tested to investigate the expansion and shrinkage strain profiles under controlled conditions in the laboratory.

Specimens were cast using the same concrete batch with that used for the industrial slabs (see Table 3.7). Three specimens were collected for each type of concrete and for both free and restrained condition specimens. The specimens were placed in a controlled room with a temperature of 27°C and 70% relative humidity.

Restrained strain profiles are important for the study of both normal and expansive concrete. The level of expansion and shrinkage depends on the degree of restraint resulted from both internal and external restraints. In order to know the level of expansion and shrinkage, many experimental cases are required for the respective degree of restraints for different mix proportions. Since many preparations are required to conduct experiments, FE analysis becomes an efficient tool to investigate the level of restrained expansion and shrinkage strain profiles of concrete. In this study, FE analysis is used to predict expansion and shrinkage strain profiles under internal restraint condition for different mix proportions.

3.5.1 Finite element modelling

LS-DYNA finite element (FE) code was used for simulating the expansion and shrinkage strain profiles of the specimens under restrained conditions. In this FE analysis, a model is composed of solid elements: concrete specimen, base slab and steel end plates and beam element: reinforcing bar. A mesh size of 1 cm was used for both solid and beam elements.

3.5.1.1 Material models for concrete and reinforcement

MAT_CONCRETE_DAMAGE_REL3 available in LS-DYNA code was used as the concrete material model in this study. The required inputs for this material model are density, Poisson's ratio and the unconfined compressive strength of concrete, and the code will generate other parameters automatically. The background theory of this concrete model is provided in detail by (Schwer & Malvar, 2005; Wu, Crawford & Magallanes, 2012). This material model was used to model both specimens and base slab with respect to their input material properties.

MAT_THERMAL_EXPANSION is an arbitrary material model to input thermal expansion coefficients of the material. This material card can be used to simulate the volume change of the material due to temperature change for both isotropic and anisotropic materials.

MAT_PIECEWISE_LINEAR_PLASTICITY, an elastoplastic material model, is employed to model the reinforcing bar. The input parameters for steel are the yield strength of 12 mm diameter bar of 513 MPa, Young's modulus of 200 GPa, and Poisson's ratio of 0.3.

3.5.1.2 Applied loadings

In order to apply free strain to the model, the relation between strain (ϵ) and temperature change (ΔT) was used to obtain the equivalent temperature. The equivalent temperature was converted from free expansion and shrinkage strains of the free condition specimens. The coefficient of thermal expansion of concrete (α_c) is adopted to be $10\mu\epsilon/^\circ\text{C}$ (Richardson et al., 2010). The applied equivalent temperature profiles (from $\Delta T = \epsilon/\alpha_c$) were shown in chapter 4 (Figure 4.28). It is noted here again that the free strain was measured 1 day after concrete casting; therefore, the equivalent temperature loading was applied to the model from day 1. Apart from applying equivalent temperature load to the concrete, the self-weight of the specimen was applied as a body load.

3.5.1.3 Boundary conditions

A 3D FE model of a restrained specimen is shown in Figure 3.15. These boundary conditions were applied in the model.

- (i) Restraint in three directions ($U_x=U_y=U_z=0$) at the joint between the endplate and reinforcing bar as endplates and reinforcing bar were locked with nuts and washers.
- (ii) Restraint in three directions ($U_x=U_y=U_z=0$) at the bottom face of the base slab as concrete specimens were placed on the concrete floor in the laboratory.
- (iii) As the specimens were placed on the concrete floor, a frictional restraint is needed to account for the analysis. Therefore, the surface to surface contact card was used to model frictional restraint from the base slab. The friction coefficients between steel endplate and concrete specimen and between the concrete specimen and base slab are 0.1 and 0.4, respectively (Gorst, Williamson, Pallet & Clark, 2003).
- (iv) A constrained beam in solid function was used to model the bond between concrete and reinforcing bar.

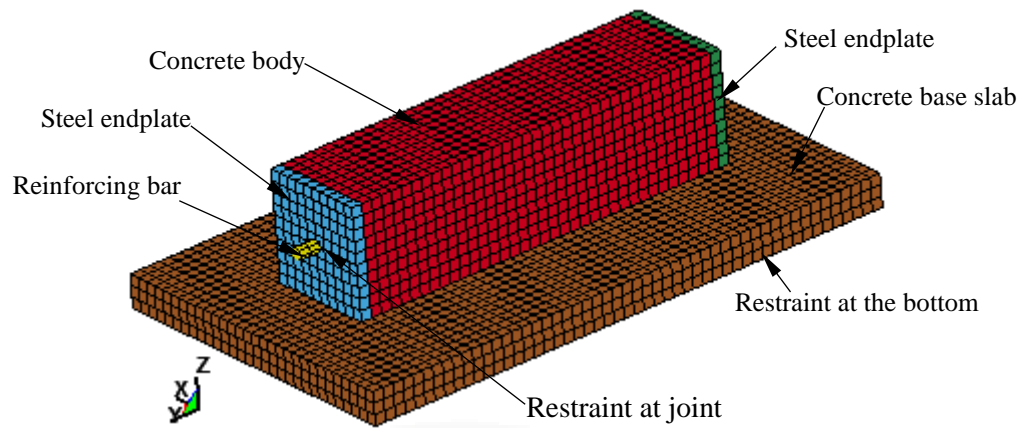
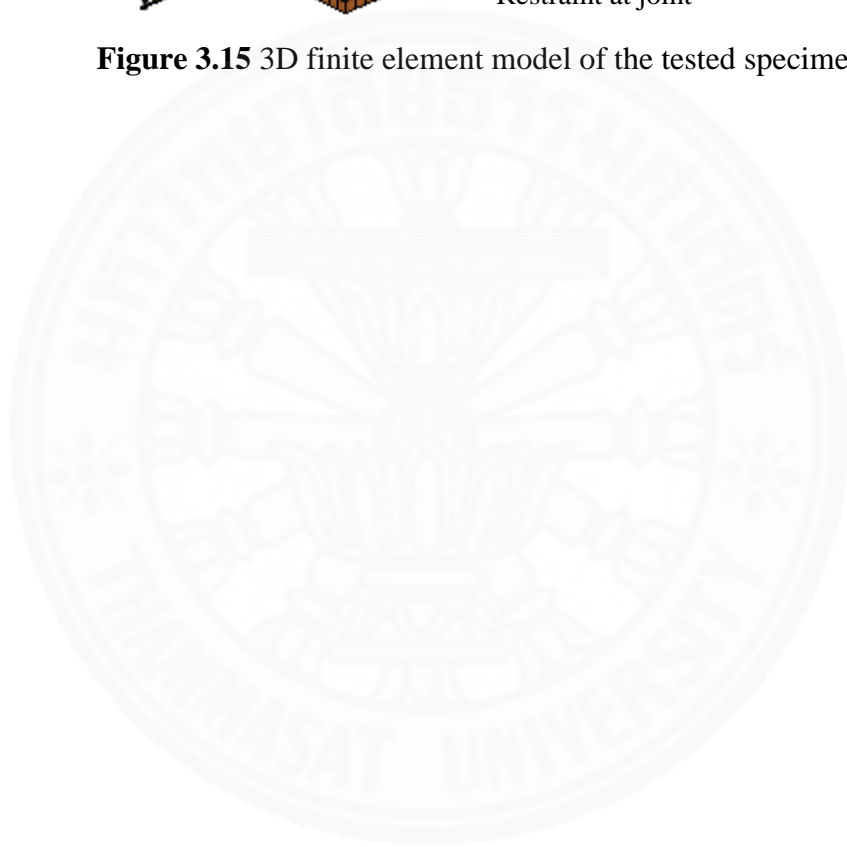


Figure 3.15 3D finite element model of the tested specimen



CHAPTER 4

RESULTS AND DISCUSSIONS

4.1 General

This chapter presents the experimental and finite element results of the studied specimens and structures as described in the previous chapter. The tests for basic material properties, i.e. compressive strength, tensile strain capacity test and modulus of rupture were conducted for all types of concrete used for the structures were investigated in this study. Moreover, the measured strain profiles from slabs on beams and footings, water tank walls, slab on grade (pavement), and industrial floor slabs were discussed with respect to internal and external restraints. Additionally, free and restrained strains of specimens were tested in the laboratory. Lastly, restrained strain profiles of specimens were predicted by using finite element analysis.

4.2 Laboratory experiment results

Tested specimens for compressive strength, tensile strain capacity as well as modulus of rupture were collected from the same concrete batch used for the real monitored structures. The compressive strength, tensile strain capacity of concrete and modulus of rupture used for slab on beam and foundation, water tank walls, slab on grade (pavements), and industrial floor slabs are summarized in Table 4.1, Table 4.2 and Table 4.3, respectively.

4.2.1 Compressive strength and tensile strain capacity tests results

The compressive strength of concrete used for slabs, water tank walls, pavements, and industrial floor slabs are summarized in Table 4.1. According to the test data, normal concrete shows higher compressive strength than the expansive concrete.

The tensile strain capacity was calculated from the flexural cracking strain obtained from the bending test. The conversion of flexural cracking strain to tensile strain capacity is shown in Equation (4.1) (Wee, Swaddiwudhipong & Lu, 2000). The calculated results of tensile strain capacity are presented in Table 4.2.

$$\varepsilon_{tsc,direct} = 0.7 \times \varepsilon_{cr,flexural} \quad (4.1)$$

Where,

$\varepsilon_{tsc,direct}$ = tensile strain capacity, μ

$\varepsilon_{cr,direct}$ = flexural cracking strain, μ

The modulus of rupture for all structural members was calculated based on ASTM C78/C78M-08 as given in Table 4.3. The calculation is based on the maximum applied load and the dimension of the specimen. The equation for the calculation of modulus of rupture is shown in Equation (4.2).

$$R = \frac{PL}{bd^2} \quad (4.2)$$

Where,

R = modulus of rupture (MPa)

P = maximum applied load (N)

L = length of specimen (mm)

b = average width of specimen (mm)

d = average depth of specimen (mm)

Table 4.1 Compressive strength of concrete in all structural members

No.	Structural Members	Name	Compressive Strength (MPa)			
			1 days	3 days	7 days	28 days
1	Slab on beam and foundation	NC-slab	12.40	21.57	25.03	30.05
		EA-slab	12.32	18.67	23.38	29.18
2	Water tank wall	EA-WT	20.33	22.42	24.16	28.93
3	Slab on grade (pavement)	NC-Pave	9.37	12.54	16.74	23.43
		EA 1-Pave 1	8.02	11.70	14.26	19.19
		EA 2-Pave 2	8.22	12.12	14.86	20.31
		EA 3-Pave 3	8.96	14.24	17.08	19.22
4	Industrial floor slab	NC-Islab	17.32	19.88	34.43	40.23
		EA 1-Islab 1	13.55	15.57	18.11	26.37
		EA 2-Islab 2	16.31	20.80	26.80	32.38

Table 4.2 Tensile strain capacity of concrete in for all structural members

No.	Structural Members	Name	Tensile Strain Capacity ($\mu\epsilon$)			
			1 days	3 days	7 days	28 days
1	Slab on beam and foundation	NC-slab	102.67	107.02	126.97	138.38
		EA-slab	88.37	97.02	105.49	118.91
2	Water tank wall	EA-WT	80.38	108.51	129.50	173.31
3	Slab on grade (pavement)	NC-Pave	95.07	110.37	126.97	152.04
		EA 1-Pave 1	98.00	105.48	115.90	143.90
		EA 2-Pave 2	78.79	101.90	128.93	141.95
		EA 3-Pave 3	96.60	106.79	113.30	143.90
4	Industrial floor slab	NC-Islab	89.86	96.94	129.80	179.42
		EA 1-Islab 1	116.99	130.79	134.07	162.35
		EA 2-Islab 2	96.61	113.04	114.36	171.54

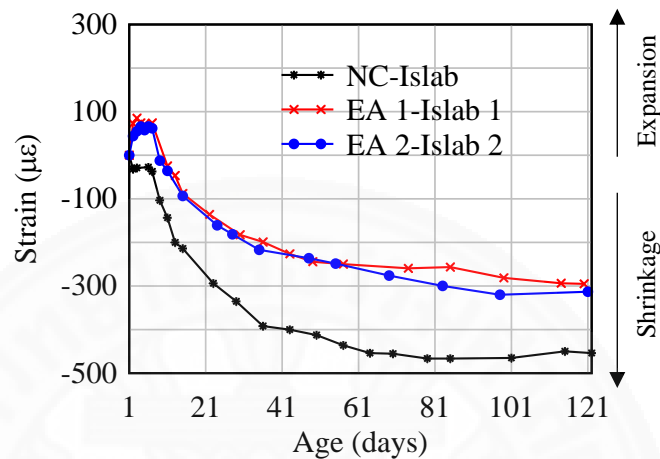
Table 4.3 Modulus of rupture of concrete in for all structural members

No.	Structural Members	Name	Modulus of Rupture (MPa)			
			1 days	3 days	7 days	28 days
1	Slab on beam and foundation	NC-slab	4.29	4.44	5.61	5.63
		EA-slab	5.05	4.19	4.92	5.25
2	Water tank wall	EA-WT	4.18	5.29	6.2	6.15
3	Slab on grade (pavement)	NC-Pave	3.45	3.64	4.77	6.31
		EA 1-Pave 1	2.36	3.63	3.7	6.11
		EA 2-Pave 2	2.27	3.53	4.21	5.07
		EA-Pave 3	-	3.71	4.37	4.98
4	Industrial floor slab	NC-Islab	4.65	5.42	5.29	6.36
		EA 1-Islab 1	2.94	3.45	3.96	4.53
		EA 2-Islab 2	3.27	3.9	4.57	5.56

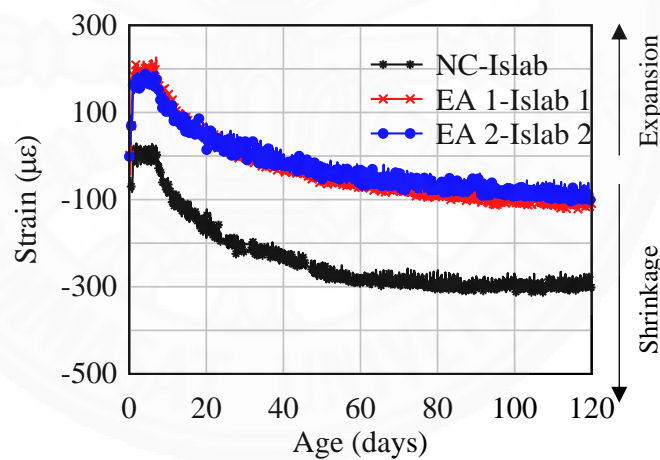
4.2.2 Experimental results of laboratory specimens

The experimental results of free and restrained specimens show that normal concrete specimens resulted in the highest shrinkage strains (see Figure 4.1). The starting measurement days between free and restrained conditions specimens were one day different. It is noted that the length change measurement for free condition specimens was performed after 1 day of casting. However, the strain measurement for the restrained specimens was performed using strain gauges connected with data logger since day 0 (day of casting). As a result, the values of free expansion strain were lower

than the values of the restrained expansion strain in the first few days as shown in Figure 4.1 (a) and Figure 4.1 (b). Additionally, the EA 1-Islab 1 and EA-Islab 2 showed the same level of expansion, although the amount of EA 1-Islab 1 is higher than EA 2-Islab 2. Therefore, EA 2-Islab 2 is more effective to produce expansion than EA 1-Islab 1.



(a)



(b)

Figure 4.1 Expansion and shrinkage strains (a) free condition (b) restrained condition

4.3 Measurement results of SIIT new laboratory building

Strain and temperature measurements of slabs (on beam and foundation), water tank walls, and slabs on ground (pavements) were carried out during the construction period of the SIIT new laboratory building. Strain gauges and thermocouples were installed at the selected locations before casting of concrete. Due to several uncontrollable factors, several data of strain and temperature were lost during the

construction. In this research, the measured strain is the total strains which are a combination of concrete expansion, autogenous shrinkage, drying shrinkage, thermal strain, creep strain, and strain from all possible loading during the construction.

4.3.1 Measurement results of slabs on beams and footings

Strain and temperature profiles of the expansive concrete slab (EA-slab) and normal concrete slab (NC-slab) were measured at the selected locations (see Figure 3.5). Data were collected and recorded using a data logger. The data were taken every 30 minutes during the measurement period of 91 days. Only some reliable data from each slab can be presented due to damaged cables or strain gauges detachment during concrete casting.

4.3.1.1 Measurement results of EA-slab

The reliable measurement data was collected from location 4, which is at the centre between two footings of the expansive concrete slab (see Figure 3.5). The strain data were measured at the mid-depth of the slab, top and bottom reinforcement in the longitudinal direction. Strain gauge for concrete was installed at the mid-depth of the slab, and strain gauges for steel were installed at the top and bottom reinforcement. Installation of strain gauges through a cross-section of the slab is illustrated in Figure 4.2. Additionally, thermocouple was installed at the mid-depth of the slab to record the concrete temperature variation of the slab throughout the measurement period. The measurement results of temperature and strain in concrete are shown in Figure 4.3 and Figure 4.4, respectively.

As can be seen from Figure 4.3, the peak temperature is observed during the initial stage after concrete pouring. This is due to a heat of hydration of the early-age concrete. The measured strain at location 4 shows different expansion and shrinkage strains at different depths with respect to their boundary conditions (see Figure 4.4). Due to high moisture loss at the concrete surface, the measured strains at the top part were the lowest, which was nearly neutral strain (neither expansion nor contraction strain). This means that the shrinkage of the top part of the slab can be reduced by using expansive concrete. The strains at the mid-depth indicate the highest values. This could be resulted from less restraint from top and bottom reinforcement, as well as the

moisture loss at this location is lower than that at the level of the top rebars. Although the moisture loss near the level of bottom rebars is low, frictional restraint from the ground could prevent expansion compared to that at the mid-depth.

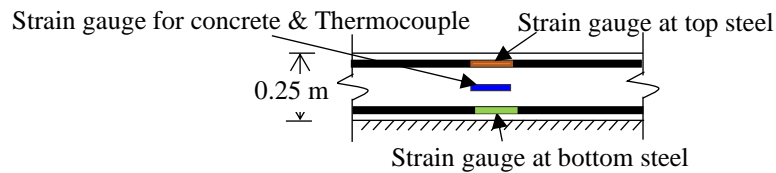


Figure 4.2 Strain gauges installation through the depth of slab

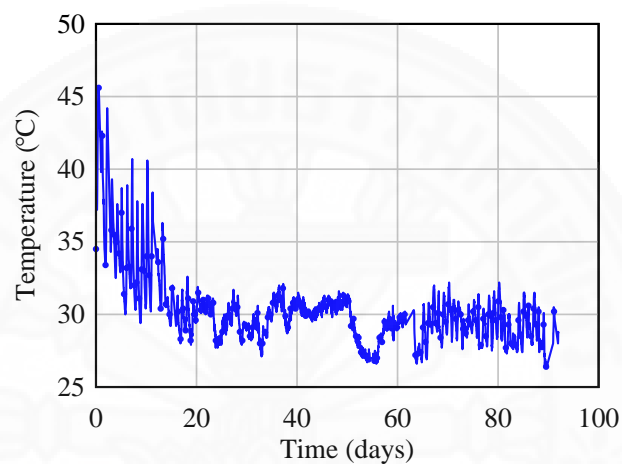


Figure 4.3 Concrete temperature measured at location 4

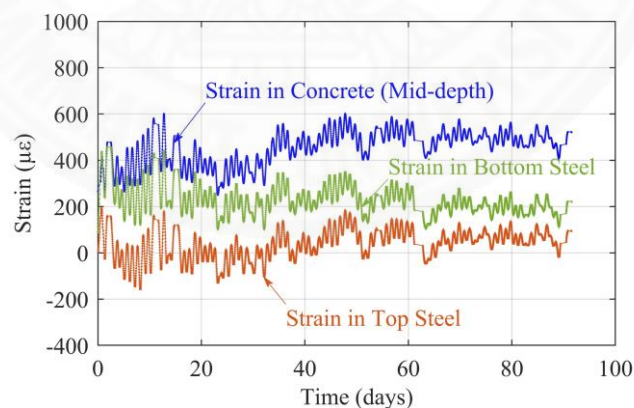


Figure 4.4 Measured strain data from the longitudinal direction of EA-slab

4.3.1.2 Measurement Results of NC-slab

In normal concrete slab, the reliable results were collected from location 9. Comparison of the strains between the expansive concrete and normal concrete slabs cannot be made as the data were from the locations with different boundary conditions.

Location 4 in the expansive concrete slab is in between two foundations, whilst location 9 in the normal concrete slab is 1 m from the centre of footing (see Figure 3.5). Therefore, the measurement results for normal concrete are not shown in this section.

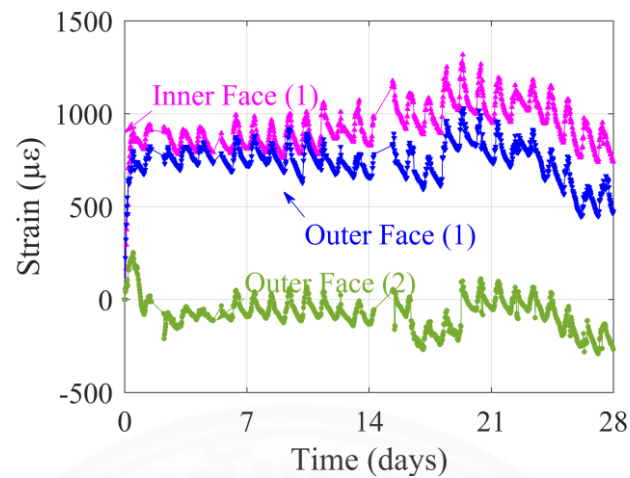
4.3.2 Measurement results of water tank walls

Four locations were selected for the east wall, and three locations were selected for the north wall to install strain gauges both in horizontal and vertical directions rebars. As the amount of reinforcements were equal for both walls, the effect of internal restraint will not be discussed here. Measurements were recorded every 30 minutes for 28 days after concrete casting.

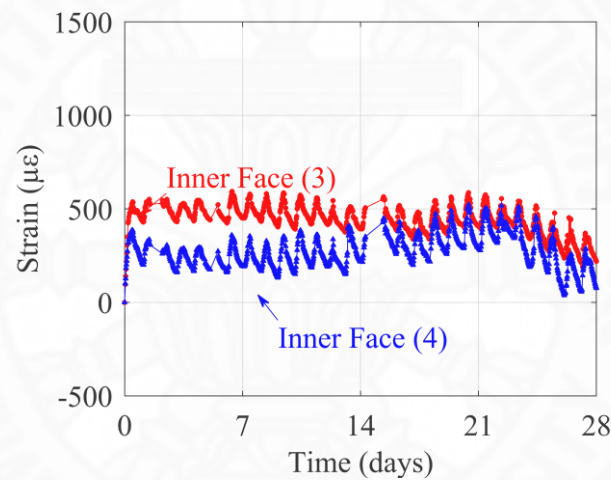
4.3.2.1 Measurement results of the east wall

From the selected locations of the east wall, the measured strain profiles from location 1 and location 2 were from the outer face of the wall, and location 3 and location 4 were from the inner face of the wall (see Figure 3.7). As the water tank was located at the rooftop of the building, the walls were highly exposed to sunlight. As a result, the measured strain profiles from the outer face of the east wall showed lower expansion strain than that of the inner face of the wall due to more severe drying at the wall surface.

The external restraints of this wall are from the base slab, top slab and side walls. Location 1 and location 3 were at the wall mid-height; as a result, there should be very small restraining effect from the base restraint. Therefore, the measured strains at these two locations were higher than those of location 2 and location 4 (see Figure 4.5). Due to high restraint from the base, the measured strains at location 2 decreased to negative values after 2 days which represented contraction strains. However, the strains of the inner face of the wall near the base (location 4) were still in compression. This is due to the fact that the moisture loss on the inner face is lower compared to that on the outer face; therefore, the used expansive concrete still shows its effectiveness to prevent the tensile stress under base restraint. However, it is noted that there is a possibility of cracking at the base of the wall on the outer face where there is a high moisture loss due to its exposure to the direct sunlight together with the high base restraint.



(a)



(b)

Figure 4.5 (a) Horizontal steel strain at location 1 and 2 of the east wall (b) Vertical steel strain at location 3 and 4 of the east wall

4.3.2.2 Measurement results of the north wall

Location 5 (mid-height), location 6 (near the base slab), and location 7 (near the top slab) were selected to investigate the strains in both horizontal and vertical directions of the outer face of the north wall (see Figure 3.8). The measured strains for both horizontal and vertical directions showed a similar trend as shown in Figure 4.6.

The restraints provided by the top and bottom slabs of the wall significantly affect the strains of location 6 and location 7 in both horizontal and vertical directions (see Figure 4.6 (a) and (b)). As a result, the measured strains at these two locations

showed lower expansion than the strains at location 5, and the strains approached negative values (contraction). However, the measured strains at the mid-height still showed high expansion in both horizontal and vertical directions due to the low degree of restraint from the top and bottom slabs at the mid-height of the wall (see Figure 4.6 (a) and (b)). To conclude from the measured strains from the walls, the effectiveness of expansive concrete can be observed as there is low tensile strain even at the location with a high degree of restraint.

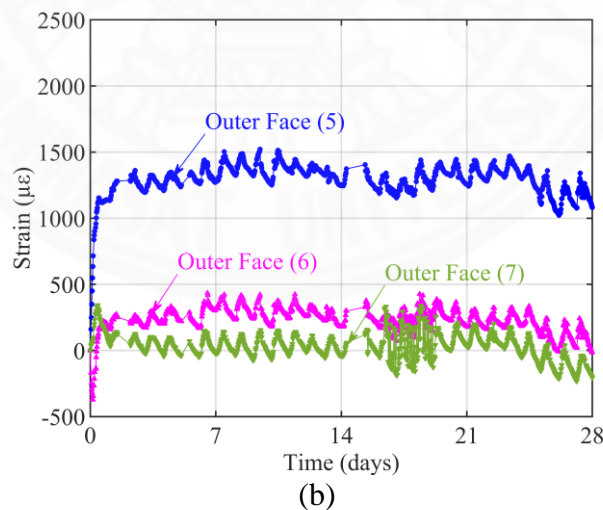
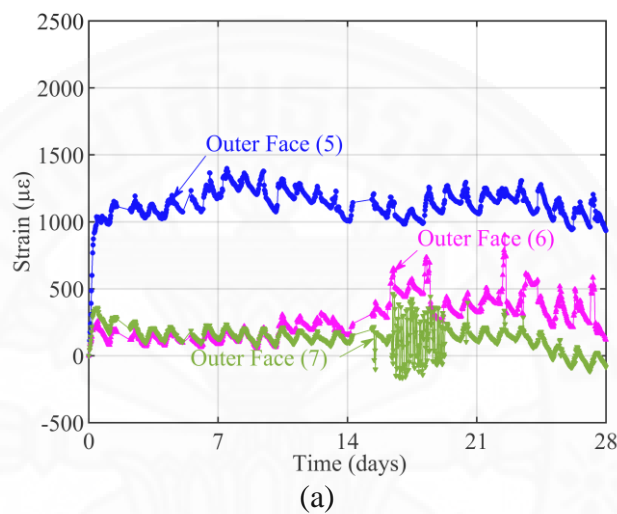


Figure 4.6 (a) Horizontal steel strain at location 5,6, and 7 of the north wall (b)
Vertical steel strain at location 5, 6, and 7 of the north wall

4.3.3 Measurement results of slab on grade (pavements)

Two locations, at the slab centre and near the expansion joint (0.6 meters from the joint), were selected to monitor the strain of the slabs (see Figure 3.10). Strain

gauges were installed in both longitudinal and transverse directions of the slab and at different depths of the slab. The strain gauges were installed at the wire mesh (35 mm from the top surface) and at the mid-depth (75 mm from the top surface). Thermocouples were installed at the mid-depth of the slab. Strain and temperature monitoring were conducted for 42 days. Unfortunately, the data at the first 7 days were lost due to some technical problems of the data logger.

The concrete temperature in normal concrete (NC-Pave), expansive concrete-1 (EA 1-Pave 1) and expansive concrete-2 (EA 2-Pave 2) slabs are shown in Figure 4.7. The temperature in EA-Pave 1 was less fluctuated as the pavement was located between two existing buildings, where there was no direct sunlight on the pavement. Also, the concrete temperature inside EA 1 -Pave 1 was lower than NC-Pave and EA 2-Pave 2 because the ambient temperature was low due to the effects of shading from two adjacent buildings.

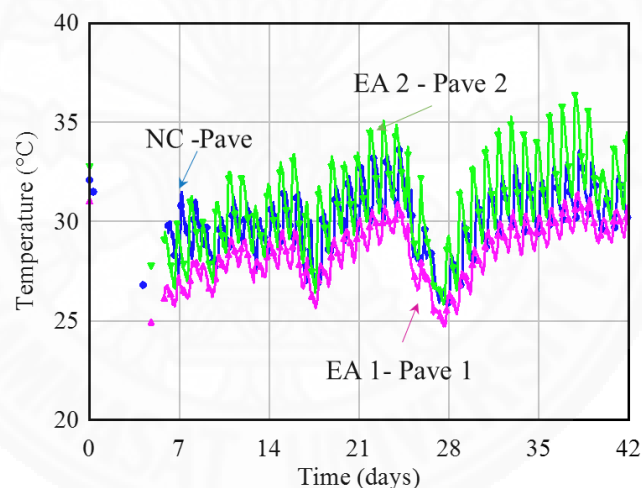


Figure 4.7 Concrete Temperature for Pavements

4.3.3.1 Longitudinal strains at mid-depth and at the level of steel layer at the centre of pavements

The locations of strain gauges through a cross-section of the pavement are shown in Figure 4.8. In this section, the measured strains in the longitudinal direction at mid-depth and at the level of steel layer are discussed. The recorded strain data are illustrated for each type of slab, as shown in Figure 4.9. From Figure 4.9, the strains at the level of steel layer are lower than those at the mid-depth. This implies that

moisture loss near the surface and the restraint from the reinforcement lead to lower expansion strains. Furthermore, the strains at the level of steel layer of NC-Pave approach contraction strain after 28 days while strains at the level of steel layer of EA pavements are still in expansion strain. This means that the used of EA in the slab is effective to compensate contraction strains resulted from concrete shrinkage. For all EA slabs, EA 2-Pave 2 shows the highest expansion both at mid-depth and at the level of steel layer, although the same EA content was used in all EA slabs. This indicates that EA 2-Pave 2 is more effective to produce expansion.

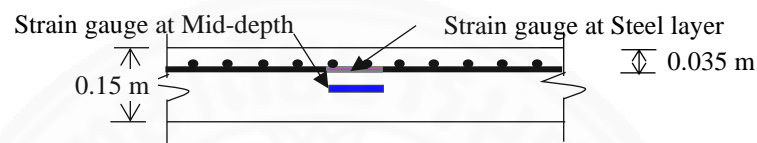
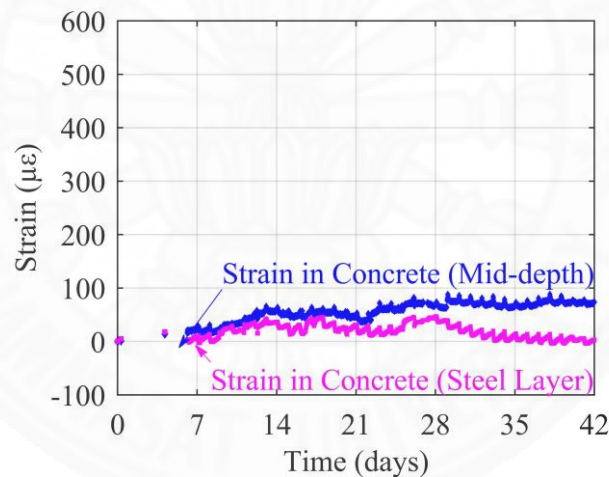
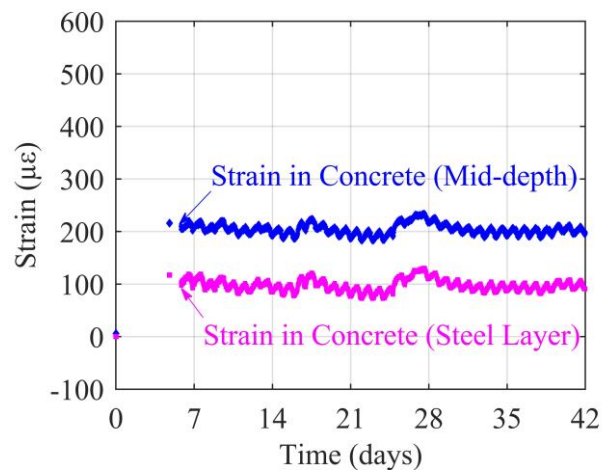


Figure 4.8 Locations of installed strain gauges in the section of pavement



(a)



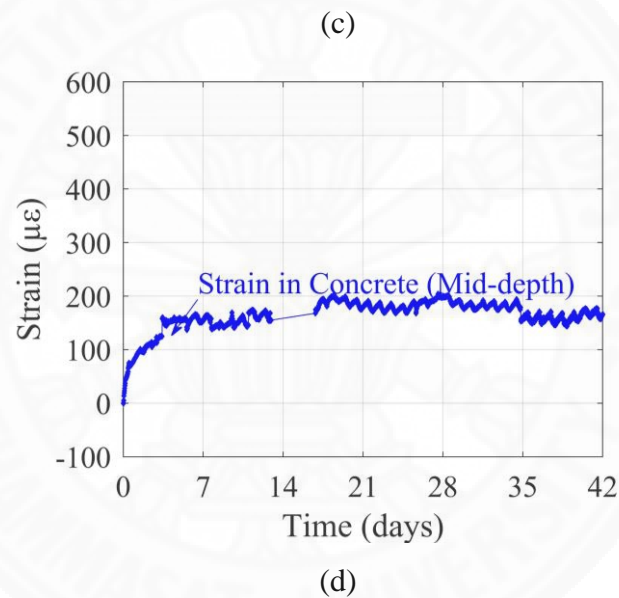
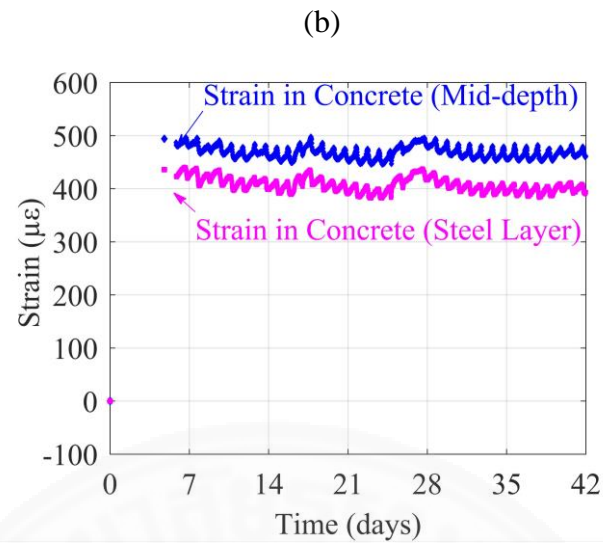


Figure 4.9 Longitudinal strain in concrete at mid-depth and at steel layer (a) NC-Pave (b) EA 1-Pave 1 (c) EA 2-Pave 2 (d) EA 3-Pave 3

4.3.3.2 Measured strain results in longitudinal and transverse directions at the centre of pavements

The strains were monitored in both longitudinal and transverse directions at the level of the steel layer. A typical plan view of the slab with the direction of the measured strain is shown in Figure 4.10. The comparison of the measured strains in both longitudinal and transverse directions in 4 types of slabs is presented in Figure 4.11. For this type of pavement structure, the frictional restraint from the base plays a vital

role due to crush rock base under the slabs. The frictional length is smaller in the transverse direction compared to that in the longitudinal direction of the slab. As a result, the degree of restraint in the transverse direction is lower. This leads to higher expansion strains in both concrete and steel in the transverse direction than those in the longitudinal direction which has a larger frictional length of the pavement. Firstly, the strains in normal concrete slab (NC-Pave) are analysed (see Figure 4.11 (a)). The expansion strain in the transverse direction is higher than that in the longitudinal direction during the first 28 days due to lower restraining effect in the transverse direction. However, the trend of the strains changed after 28 days significantly. The strain in the transverse direction decreased to negative values (contraction strain). This shows that normal concrete slab started to shrink after 28 days in the transverse direction while strain in the longitudinal direction of the pavement approached neutral strain ($0 \mu\epsilon$). Secondly, strains in EA-paves are investigated from Figure 4.11 (b), (c) and (d). All the results showed the positive values (expansion strains) during the measurement period. These results confirm that the use of expansive concrete is effective to compensate restrained contraction strain caused by concrete shrinkage.

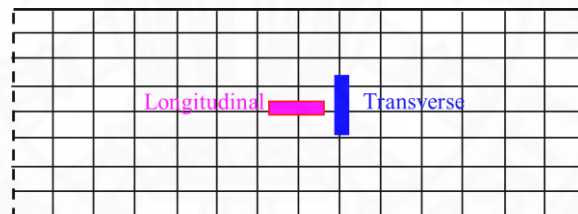
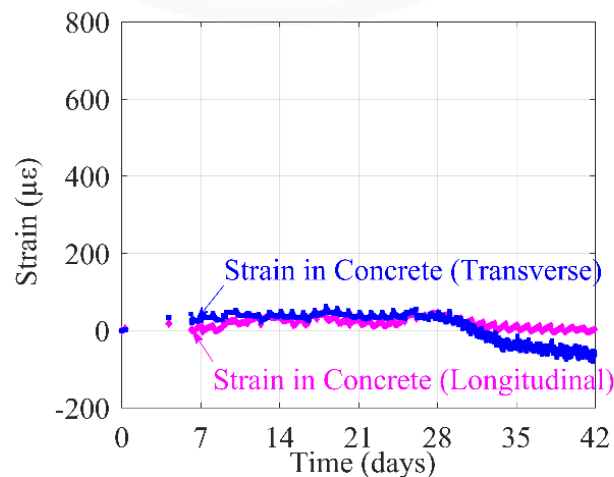
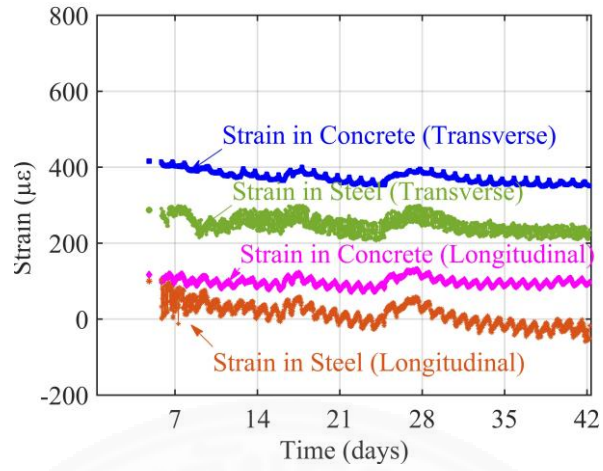


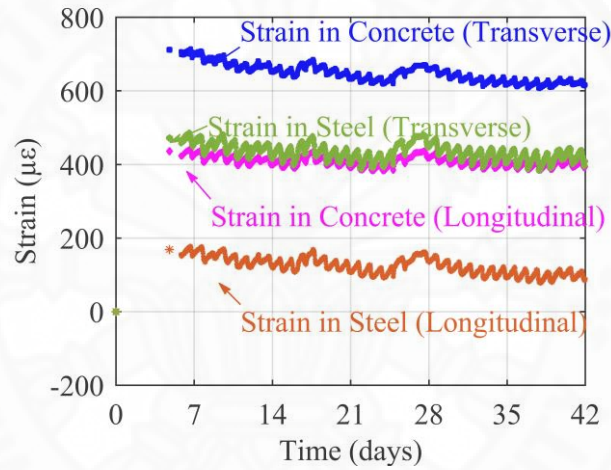
Figure 4.10 Layout of installed strain gauges at the centre of pavement



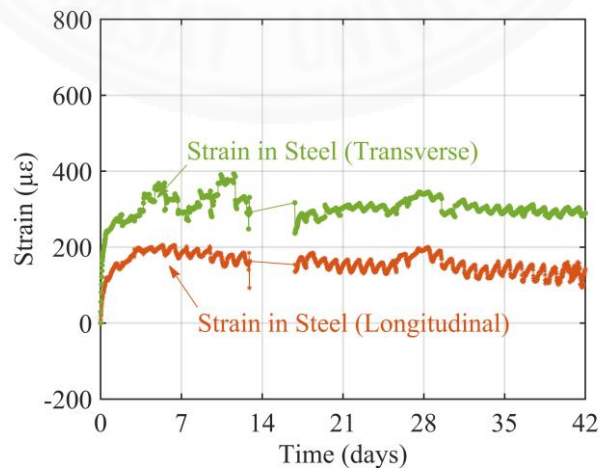
(a)



(b)



(c)



(d)

Figure 4.11 Longitudinal and transverse strain profiles at the slab centre (a)NC-Pave (b)EA 1-Pave 1 (c) EA 2-Pave 2 (d) EA 3-Pave 3

4.3.3.3 Longitudinal strains at centre and joint of pavements

Strain gauges were installed at the centre and near an expansion joint of each pavement in order to observe different degrees of restraint in these two locations (see Figure 4.12). The measured strain data near a joint in EA 1-Pave 1 was not available since strain gauges in this location were damaged during the concrete casting. The measured longitudinal strain data for NC-Pave, EA 2-Pave 2 and EA 3-Pave3 are shown in Figure 4.13. From Figure 4.13 (a), the strains at the joint of the pavement showed the contraction strain (shrinkage) during the measurement period while the measured strain at the centre part was still in small expansion until 33 days of age. This implies that the high restraint near the joint resulted in contraction strain in normal concrete pavement. On the other hand, expansive concrete pavements (EA 2-Pave 2, EA 3-Pave 3) show the expansion strains for both centre and joint parts of the pavements (see Figure 4.13 (b) and (c)). This implies that the advantage of using expansive concrete can be observed as the expansion strains can be seen at the high restraint part in EA slabs.

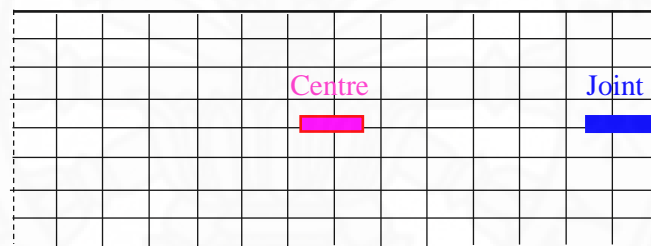
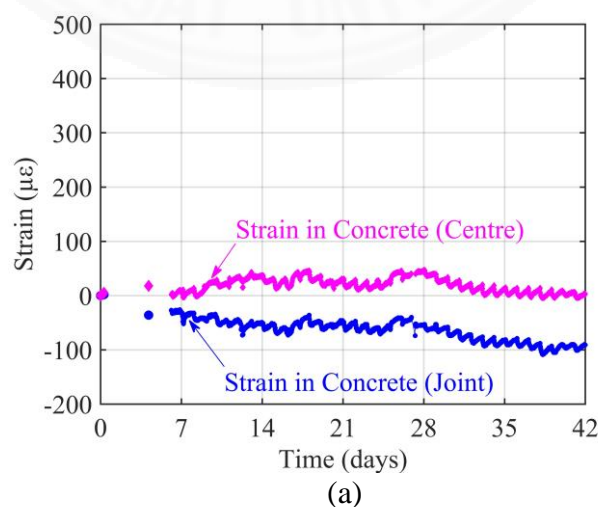
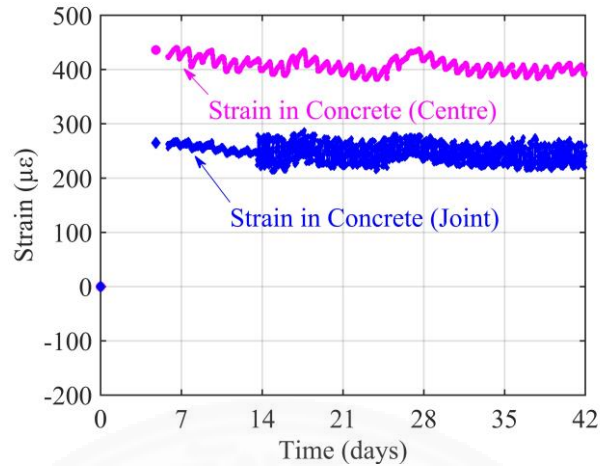
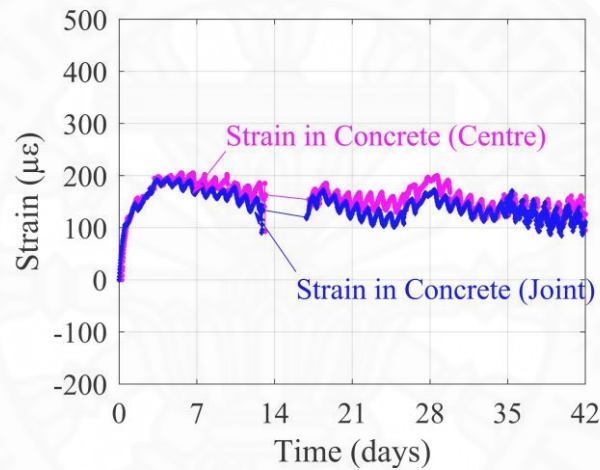


Figure 4.12 Strain gauges layout at centre and joint of pavement





(b)



(c)

Figure 4.13 Longitudinal strain in concrete at centre and joint (a) NC-Pave (b) EA 2-Pave 2 (c) EA 3-Pave 3

4.4 Measurement results of industrial floor slabs (Islab)

Strains and concrete temperature were measured in industrial floor slabs (slabs on beams and footings). Normal concrete (NC) and two types of expansive concrete (EA) were used for casting three monitored slabs. The possible restraints which could affect the slab strains are reinforcement, base friction, footings, perimeter beams, ambient temperature and relative humidity.

Strain gauges were installed at the mid-depth of the slab and also at the level of top rebar. Extra rebars with the pre-installed strain gauges were prepared in advance and installed later at the construction site. It is noted that these pre-installed strain gauges were intentionally prepared for the strain measurement at the mid-depth of the

slab whilst the strain at the level of top rebar can be obtained from the strain gauges attached directly to the existing top rebar. Strains were investigated in both long and short directions of the slab.

4.4.1 Measurements results of NC-Islab

Four locations with different boundary conditions (see Figure 3.12) were selected to measure the strains. Concrete temperature was monitored at the mid-depth of the slab at location 1. The recorded concrete temperature is shown in Figure 4.14. NC-Islab was under the open roof during the first 20 days, therefore, there was large fluctuations in the measured temperature.

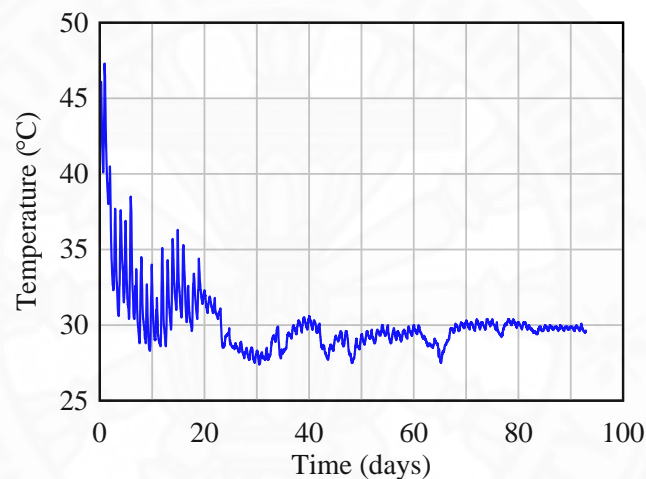


Figure 4.14 Concrete temperature in NC-Islab

4.4.1.1 Measurement results at location 1

Location 1 is in between two footings of the slab. As can be seen from Figure 4.15, the measured strains at the existing top steel showed shrinkage strain since day 0. This means that there is a higher moisture loss at the surface of the slab than that at the mid-depth of the slab. Measured strain in the short direction showed a sudden change at 25 days, which might be because of the formation of crack near the strain gauge.

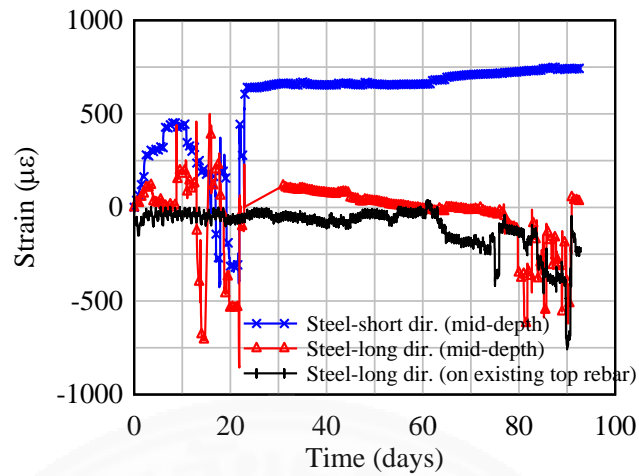


Figure 4.15 Measured strains in short and long directions at location 1

4.4.1.2 Measurement results at location 2

Location 2 is at a distance 70 cm away from the perimeter beam along the long direction of the slab. In Normal concrete, slab and perimeter beam are casted monolithically (see Figure 4.16). Therefore, the restraint from the perimeter beam is stronger along with the concrete age.

From Figure 4.17 (a), the measured strain on the top existing steel in the long direction of the slab showed an average of 0 $\mu\epsilon$ with fluctuations since there was construction loading which came from installation of floor tiles on the slab surface. From Figure 4.17 (b), the expansion stain is lower in long direction as there are restraints from base friction and perimeter beam in the long direction of the slab. Strain in short direction of the slab showed high expansion strain as the frictional area is small in short direction of the slab.

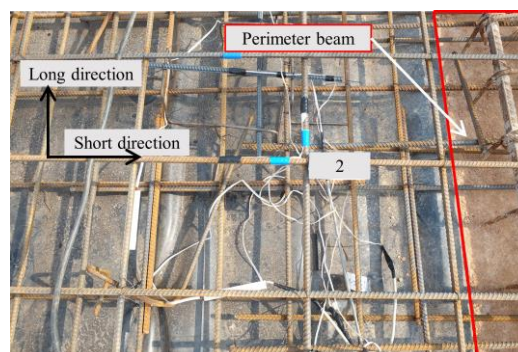
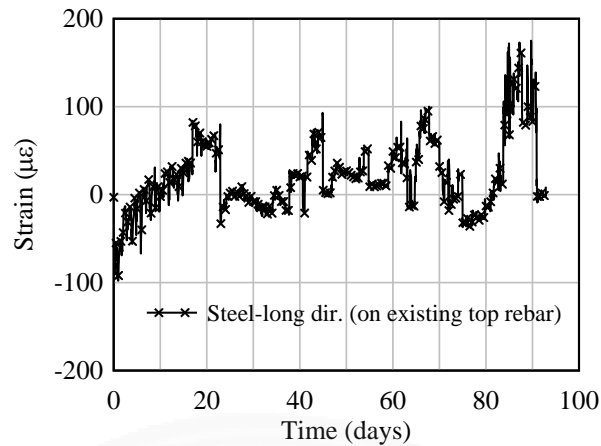
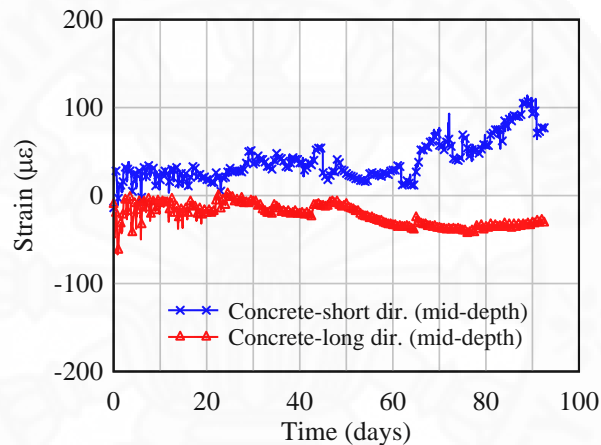


Figure 4.16 Effect of perimeter beam to location 2



(a)



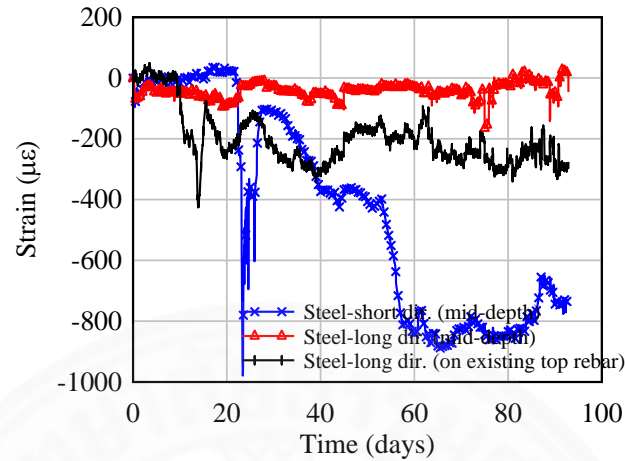
(b)

Figure 4.17 Measured strains in short and long directions at location 2 (a) at top existing steel (b) in concrete at mid-depth

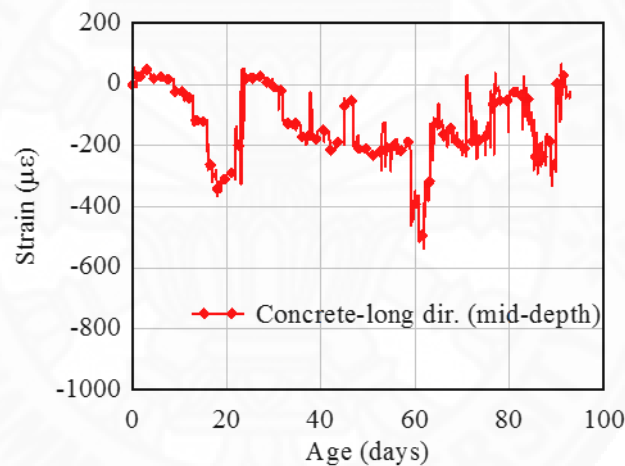
4.4.1.3 Measurement results at location 3

Location 3 is at a distance 70 cm from the perimeter beam in the short direction of the slab. According to Figure 4.18 (a), the measured strains in location 3 showed the same behaviour as in location 2. In the long direction of the slab, the measured strains at the mid-depth remained about 0 $\mu\epsilon$ and the measured strain at the existing top steel decreased to negative values which represent shrinkage in the concrete. The measured shrinkage strain in the top rebar decreased to 200 $\mu\epsilon$ after 10 days, since there was a high moisture loss at the concrete surface, which can initiate contraction strain inside the concrete under restrained condition. However, the measured strains in the short

direction of the slab showed higher shrinkage than the long direction of the slab as there is less restraint in the short direction.



(a)



(b)

Figure 4.18 Measured strains in short and long directions at location 3 (a) in steel (b) in concrete at mid-depth

4.4.1.4 Measurement results at location 4

Location 4 is at the right corner of the slab, which is at a distance 70 cm away from both short and long direction perimeter beams. At this location (see Figure 4.19), the behaviour of measured strains of steel and concrete in both short and long directions of the slab were similar to those at location 2 and location 3. As long direction has a high degree of restraints due to long continuity and base friction, concrete shrinkage can maintain at 0 $\mu\epsilon$ after 40 days while concrete shrinkage gradually increases along with the time and reached -200 $\mu\epsilon$ (contraction strain) at the age of 45 days in the short

direction of the slab. This implies that there is a less degree of restraint in the short direction to suppress concrete from shrinking under restrained condition.

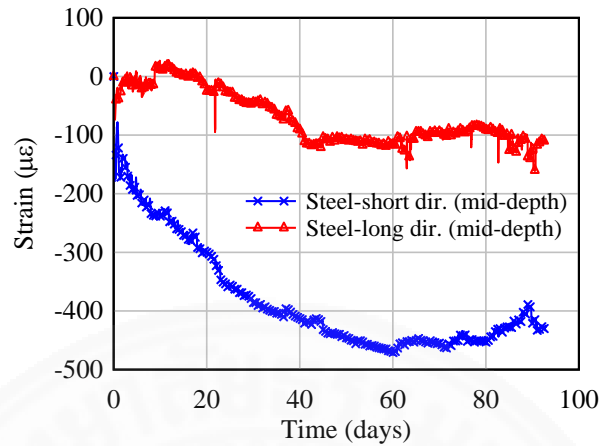


Figure 4.19 Measured strains in short and long directions at location 4

4.4.2 Measurements results for EA 1-Islab 1

Three locations were selected to investigate the strains and temperature of the slab constructed using expansive concrete. The measurement was conducted for 91 days. The selected measured locations were previously shown in Figure 3.13. The external boundary conditions of EA 1-Islab 1 were one adjacent slab in short direction and two adjacent slabs in the long direction, as shown in Figure 3.11. The concrete temperature was measured at the mid-depth of the slab at location 8. The concrete temperature reached a peak after 7 hours of casting due to the hydration reaction. The concrete temperature gradually decreased to about 30°C after ten days of casting, as shown in Figure 4.19.

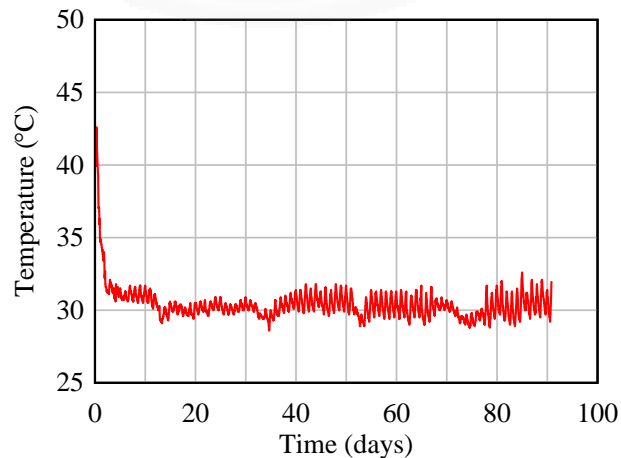


Figure 4.20 Concrete temperature in EA 1-Islab 1

4.4.2.1 Measurement results at location 7

Location 7 is at a distance 70 cm from the short direction perimeter beam (see Figure 3.13). In EA 1-Islab 1, perimeter beam casted before slab (see Figure 4.21). Therefore, friction is formed between EA 1-slab 1 and perimeter beam, which is lower restraint from the perimeter beam to location 7.

Strain gauges for steel were installed at the mid-depth and at the top existing reinforcing bar. According to the previous measurement of strains in normal concrete industrial floor slab, the measured strains from the existing rebar, which is near the top surface of the slab, showed the shrinkage strain. However, the measured strain near the top surface (on existing rebar) at location 7 in EA 1-Islab 1 showed $0 \mu\epsilon$ which was stable throughout the measurement period (see Figure 4.22). Moreover, the measured strains in the short direction from the mid-depth is still in the expansion until the end of the measurement period (91 days). This implies that the expansive concrete can reduce the shrinkage strain effectively. The measured strain in the long direction of the slab shows the expansion strain during first 38 days due to less frictional restraint from adjacent perimeter beam. The measured strain showed the shrinkage strain of $-200 \mu\epsilon$ at 91 days when frictional restraint from perimeter beam is high, however, it is still lower than the shrinkage strain of $-300 \mu\epsilon$ in NC-Islab (see Figure 4.18 (b)).

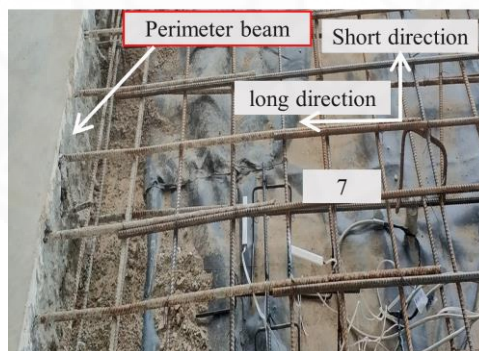


Figure 4.21 Effect of perimeter beam to location 7

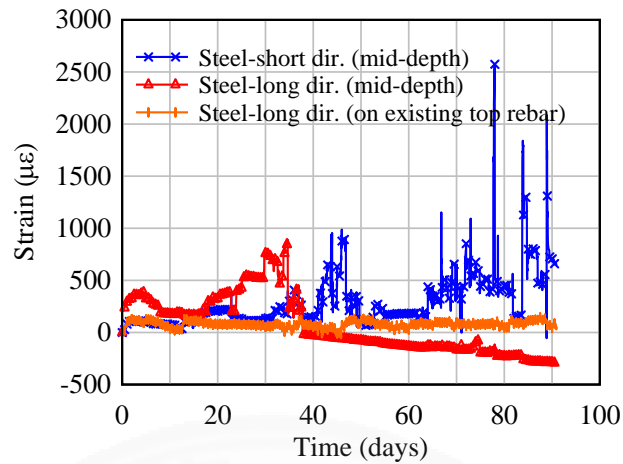
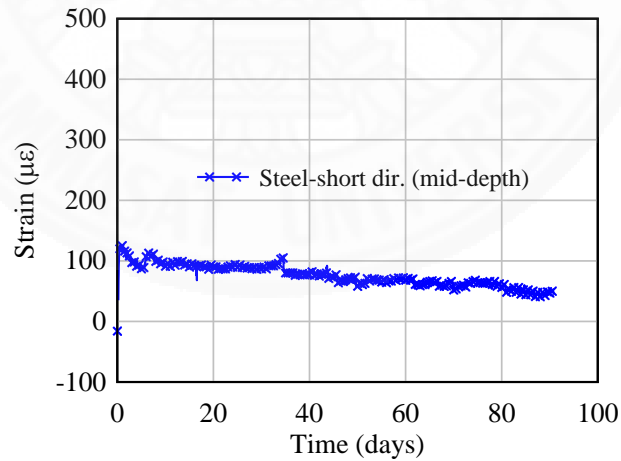


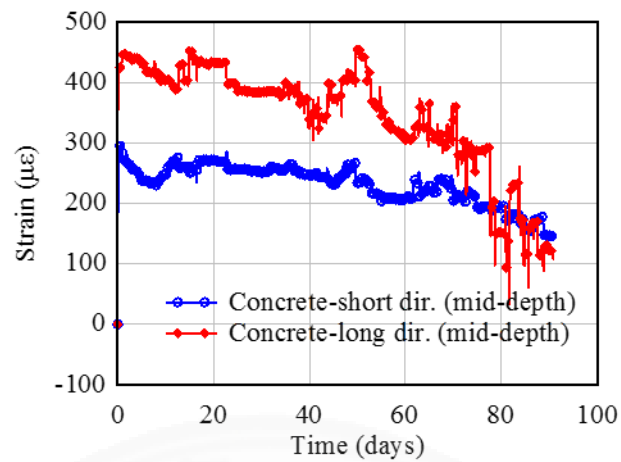
Figure 4.22 Measured strain in short and long directions at location 7

4.4.2.2 Measurement results at location 8

The measurement results of strains at location 8 are illustrated in Figure 4.23. The measured strains from both steel and concrete at the mid-depth of the slab are expansion strain until 91 days. This emphasizes that the usage of expansive concrete is also effective at this location even though this location which is highly restrained from two large adjacent footings, internal reinforcement, and base friction.



(a)



(b)

Figure 4.23 Measured strains in short and long directions at location 8 (a) in steel at mid-depth (b) in concrete at mid-depth

4.4.2.3 Measurement results at location 9

Location 9 in EA 1-Islab 1 is at a distance 200 cm from the long direction the perimeter beam. Basically, this location is in the middle of perimeter beam and adjacent footing. Therefore, it is likely to be less restrained from those adjacent structural members. The measured strains at the mid-depth from the short direction showed nearly 200 $\mu\epsilon$ expansion at 1 day and was gradually shrinking to -240 $\mu\epsilon$ at 91-day (see Figure 4.24).

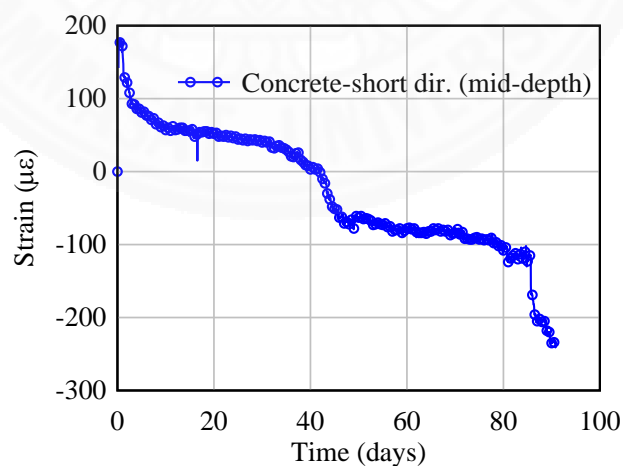


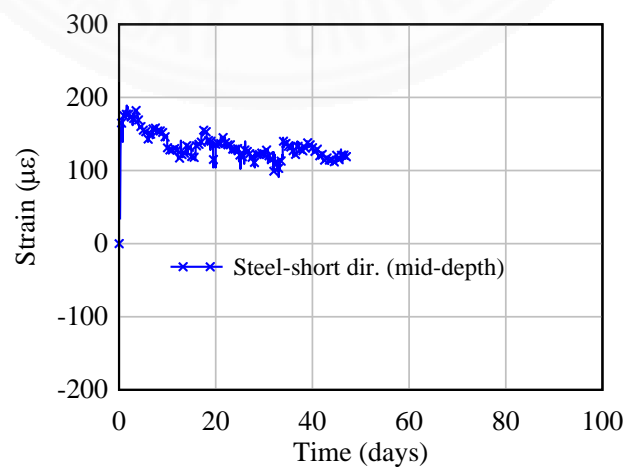
Figure 4.24 Measured strain in short direction at location 9

4.4.3 Measurements results of EA 2-Islab 2

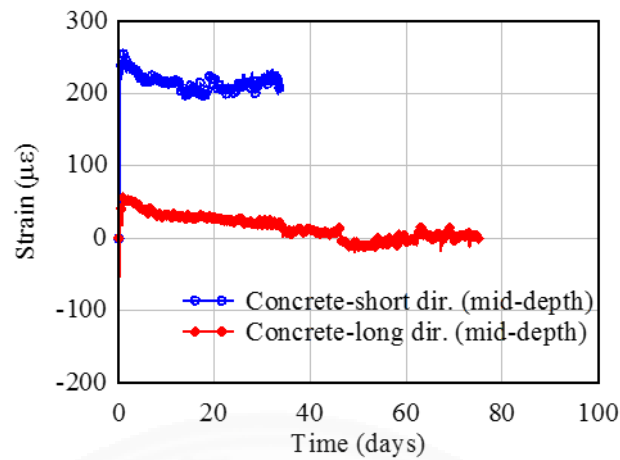
Three locations with different boundary conditions were selected to monitor the strains in EA 2-Islab 2. The concrete temperature was also monitored in this slab, but the thermocouple installed for this slab was damaged during concrete casting. Therefore, the concrete temperature was not available for this slab. The measured strains for 75 days are presented below.

4.4.3.1 Measurement results at location 10

Location 10 is located at the middle of the long perimeter beam and adjacent footings. Strain gauges for steel and concrete in the short direction stopped working after 49 days and 35 days, respectively due to some connection problems between cables and data logger. EA 2-Islab 2 was restrained on two sides: one in the long direction (from EA 1-Islab 1) and another one in the short direction from the adjacent slab (see Figure 3.11). Due to the high degree of restraint resulted from the friction in the long direction, the measured strain in long direction showed lower expansion strain than that in the short direction of the slab. From Figure 4.25, the measured strains in short direction for both steel and concrete show the compressive strains with the maximum expansion value of $180 \mu\epsilon$ and $250 \mu\epsilon$, respectively. Moreover, $0 \mu\epsilon$ can be observed in the long direction (high degree of restraint direction) of the slab (see Figure 4.25 (b)). This means that using expansive concrete is effective in this kind of restrained slab.



(a)

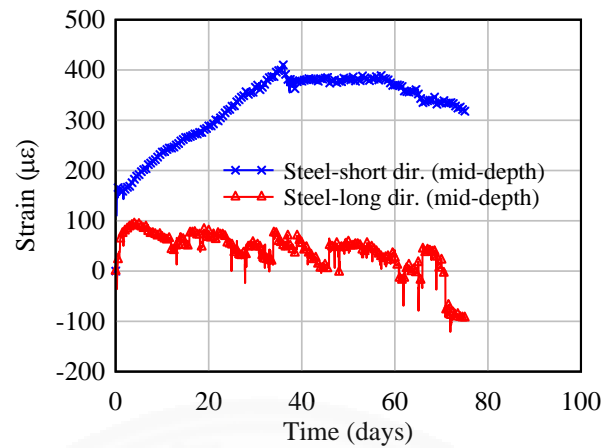


(b)

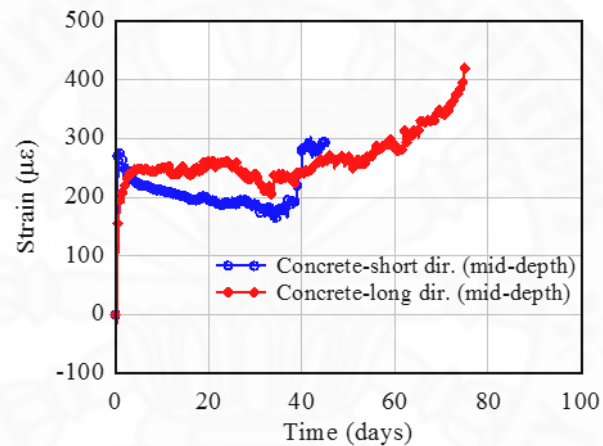
Figure 4.25 Measured strain in short and long directions at location 10 (a) in steel at mid-depth (b) in concrete at mid-depth

4.4.3.2 Measurement results at location 11

Location 11 is between two footings in the slab. The measurement results of this location show the same behaviour as location 10. From Figure 4.26, the high expansion strains can be observed in both steel and concrete in short direction of the slab as there is less restraint from base friction. The expansion strains in long direction are lower than that of short direction of the slab. This is resulted from a higher degree of restraint resulted from footings in the long direction of the slab. Moreover, it can be seen that the measured strains jumped suddenly at the age of 34 days for both steel and concrete in long direction of the slab. There could be crack formation near the strain gauges in this direction of the slab. Therefore, the measured strain data in long direction of the slab are not reliable after 34 days.



(a)

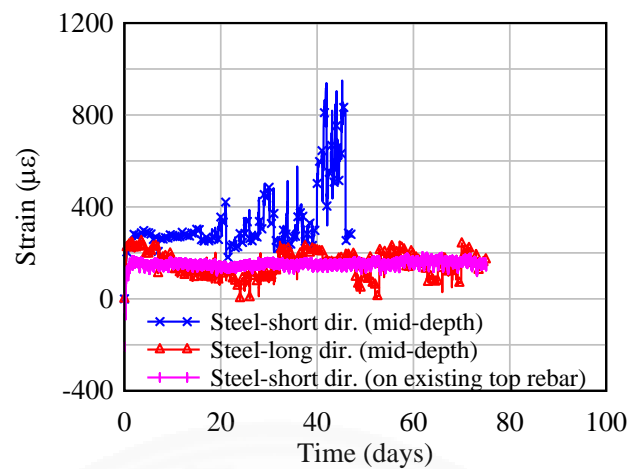


(b)

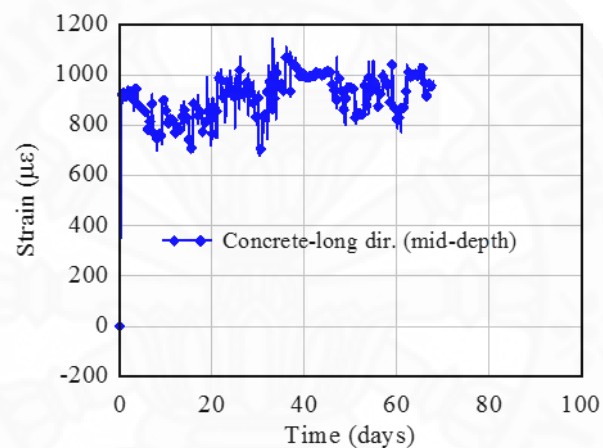
Figure 4.26 Measured strains in short and long directions at location 11 (a) in steel at mid-depth (b) in concrete at mid-depth

4.4.3.3 Measurement results at location 12

Location 12 is located at a distance 70 cm from the short direction perimeter beam. From Figure 4.27 (a), The expansion strain in the short direction of the slab is only $150 \mu\epsilon$ as a result of high moisture loss at the surface of the slab. Measured strain in mid-depth of the long direction of the slab showed expansion strain until the end of measurement period (75 days) although there is high degree of restraints from perimeter beam along the short direction and friction. All the measured strains at this location were in expansion. This proves the effectiveness of using expansive concrete to compensate the restrained contraction (shrinkage) strain.



(a)



(b)

Figure 4.27 Measured strain in short and long directions at location 12 (a) in steel (b) in concrete at mid-depth

4.5 Prediction of restrained strain in expansive concrete specimens (prisms) by Finite Element Analysis (FEA)

4.5.1 Applied loading from the experimental results

The free strains from the free condition specimens were converted into equivalent temperature profiles by using a simple relationship between strain and temperature, as shown in Equation 4.2. The equivalent temperature change history for the loadings applied in the FE models are given in Figure 4.28.

$$\varepsilon(t) = \alpha_c \Delta T(t) \quad (4.3)$$

where

$\varepsilon(t)$ = free strain from the free condition specimens

α_c = coefficient of thermal expansion of concrete

$\Delta T(t)$ = equivalent temperature change

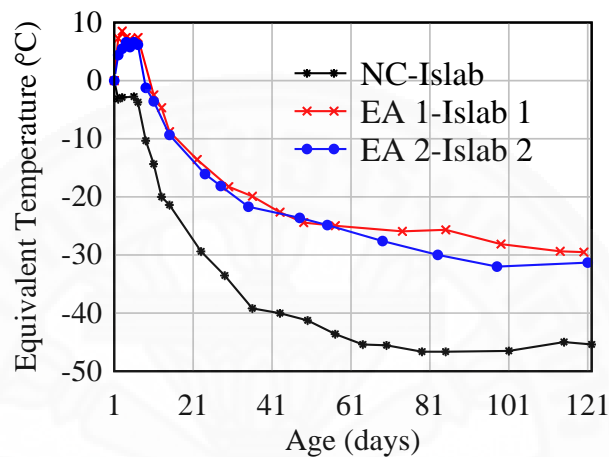


Figure 4.28 Applied equivalent temperature curves

4.5.2 FE results of restrained specimens

Initially, the prediction of steel strain was conducted by FE analysis and compared with the measured restrained strain obtained from the experiment. Thereafter, the strain contours at the mid-depth of the specimens were investigated to capture the strain distribution along the specimens.

4.5.2.1 Comparison of strain between experimental and FE results

The strains under restrained condition are shown in Figure 4.30. The early expansion strains of normal concrete are lower than $30 \mu\epsilon$, and the shrinkage strain is approximately $300 \mu\epsilon$ since 60 days of age. However, the expansion strains are about $200 \mu\epsilon$ for both expansive concrete-1 and expansive concrete-2, and the shrinkage strains for both slabs are about $100 \mu\epsilon$.

The term “effective free expansion” should be used to define the true free expansion under the restrained condition. Normally, the intrinsic free expansion under restrained condition is lower than that under unrestrained condition. This is because

some portions of the expansive crystals fill inside some of the concrete pores which cause the reduction of intrinsic free expansion under restrained condition (see Figure 4.29). However, the “effective free expansion” method was not applied in this study because the starting measurement days between free and restrained specimens are one day different, as explained in section 3.2.4. In order to discard this unknown level of effective expansion under restrained condition, the initial maximum restrained expansion strain from FE analysis was offset to be the same as the measured results. It is found out that there is a good agreement between the predicted (FE analysis) and the measurement results (see Figure 4.30).

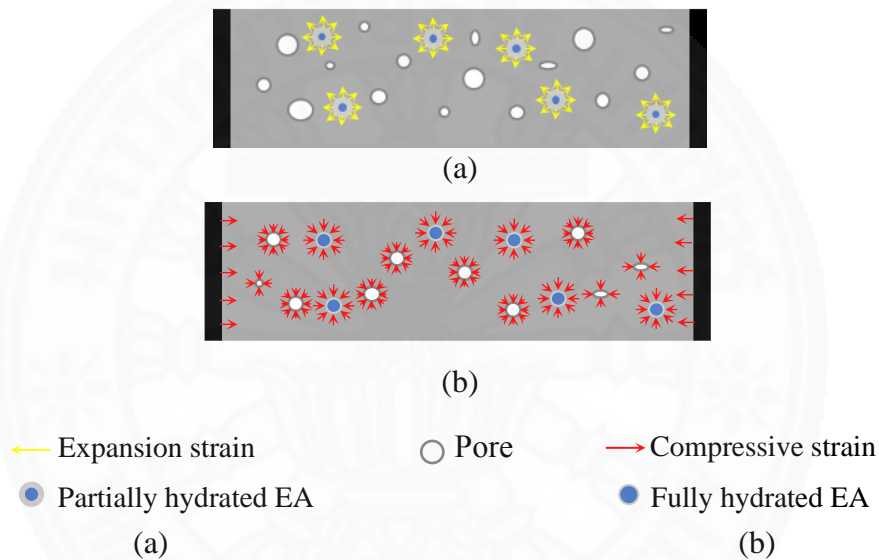
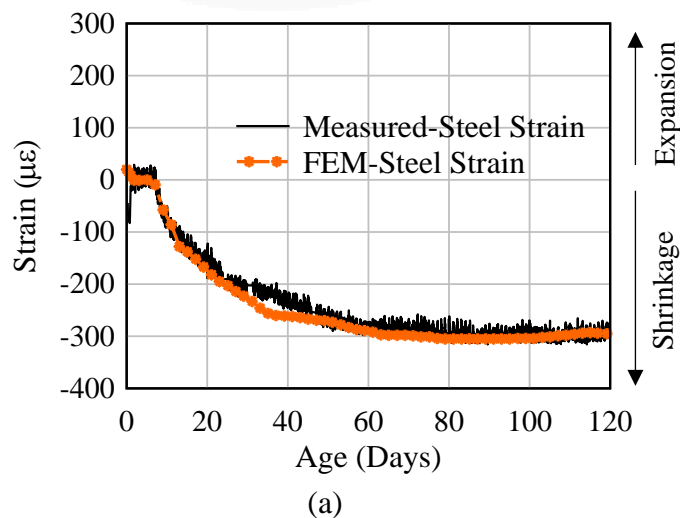
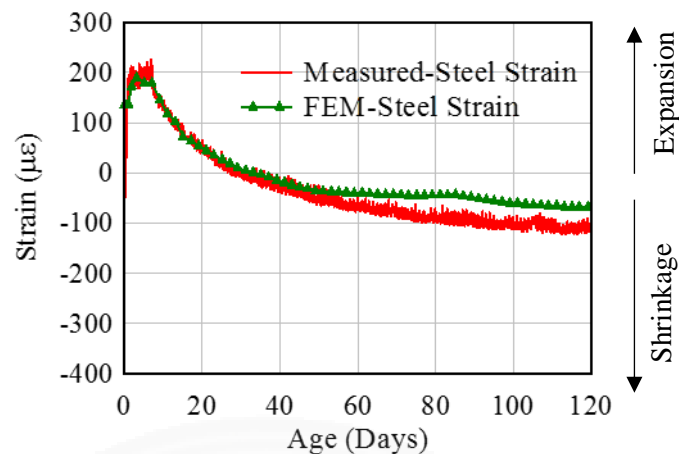
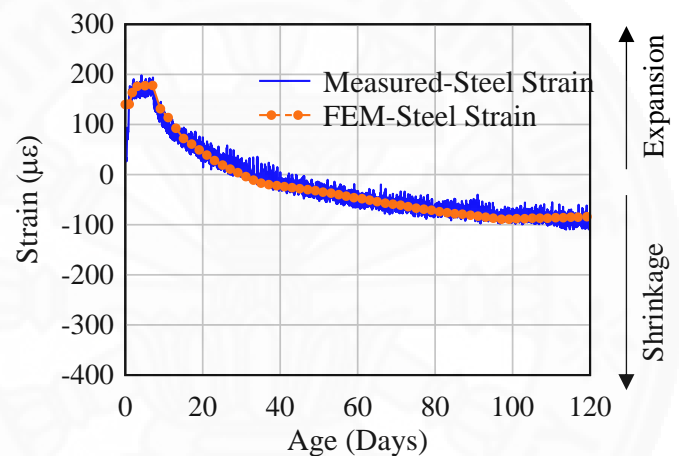


Figure 4.29 Illustration of expansive additive reaction in pore structures of concrete under restrained condition (a) partially hydration (b) fully hydration





(b)



(c)

Figure 4.30 Comparison of experimental and FE results (a) NC- Islab (b) EA 1- Islab 1 (c) EA 2- Islab 2

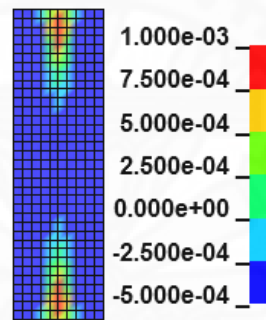
4.5.2.2 Investigation of strain distribution in restrained specimens

Contours of maximum principal strain at the mid-depth of all the specimens resulted from expansion and shrinkage strains are presented in Figure 4.31. Due to high-end restraint provided by nuts; the normal concrete specimens showed the maximum tensile strain near the end, which might lead to crack formation. However, the expansive concrete specimens still showed the less tensile strain.

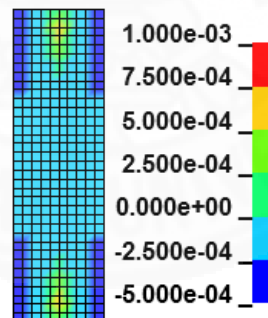
Figure 4.32 shows the different strain between those at the centre and at the end of the specimens. In all specimens, the compressive strains (negative value) are

observed at the central portion of the specimens while tensile strains (positive value) are observed at the end of the specimens. From

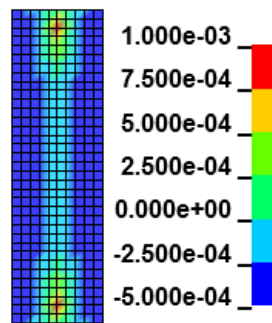
Figure 4.32 (a), the maximum tensile strain is over $1200 \mu\epsilon$ near the end of the normal concrete specimen as there are high-end restraints to the concrete from the tightened nuts on both ends. As a result, there are the possibility of initiating cracks near the end of the specimen; however, the middle part of the specimen shows the compressive strain. According to Figure 4.32 (b) and (c), the less tensile strain can be found near the end of the specimens in expansive concrete specimens. This implied that the expansion strain resulted from the expansive concrete can reduce the contraction strain resulted from the concrete shrinkage under restraint condition.



(a)

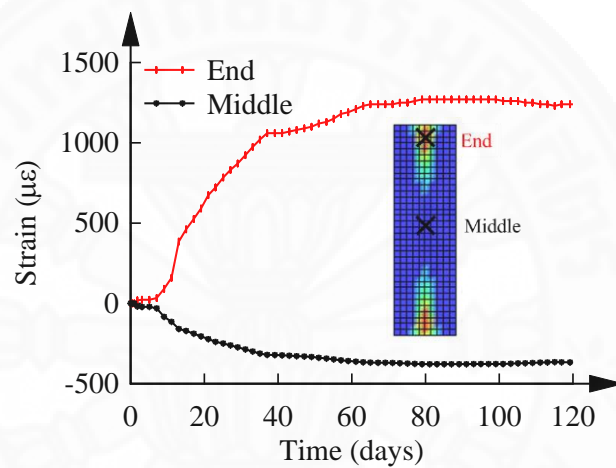


(b)

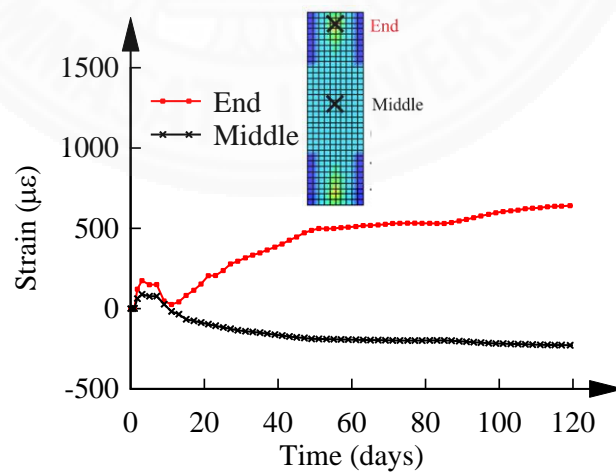


(c)

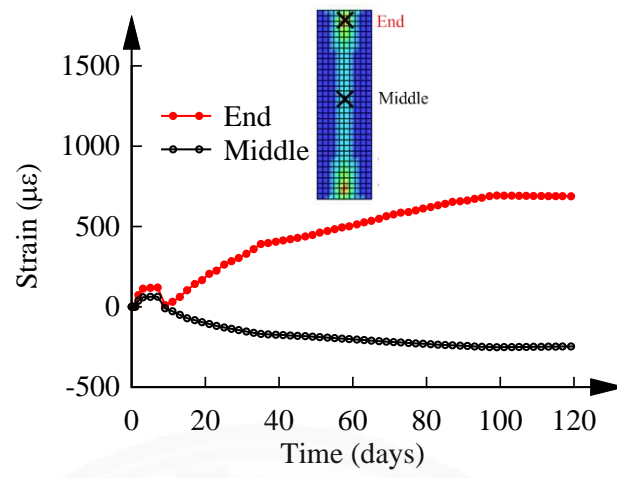
Figure 4.31 Maximum principal strain at mid-depth of the specimens (a) (a) NC-Islab (b) EA 1- Islab 1 (c) EA 2- Islab 2



(a)



(b)



(c)

Figure 4.32 Maximum principal strain at end and middle part of specimens (a) NC-Islab (b) EA 1- Islab 1 (c) EA 2- Islab 2

CHAPTER 5

CONCLUSIONS AND RECOMMENDATIONS

5.1 Conclusions

Different types of reinforced concrete structural elements such as slabs on beams and footings, slabs on ground, water tank walls, and industrial slabs. It is necessary to study these structures to know the time-dependent behaviour of restrained strains with different degree of restraints under the construction environment. Real-time monitoring of these structural elements in construction sites, basic material properties tests, free and restrained specimens in the laboratory was conducted. Additionally, restrained strains of the specimens were predicted using finite element analysis. Based on these experimental and analysis works, the following conclusions can be summarized.

1. As the water tank walls are highly exposed to the sunlight due to its location, there is a large difference in the measured strains between the outer and inner faces of the wall. It should be noted that using expansive concrete at the locations experiencing in high moisture loss together with the high restraint from the surrounding structural members can reduce the efficiency of forming compressive strain in concrete. A proper design of this kind of structure must be performed.
2. For wall structures, the restraints provided by the top and base slabs, and sidewalls as well as the effects of sunlight are the main factors affecting the level of expansion and shrinkage. Therefore, different degrees of restraint can be observed along the height and length of the wall. As a result of the high degree of restraint near the top and bottom slab of the wall, the measured strains near these locations almost reach the tensile strain capacity of the concrete. In order to design this type of structures with highly different degrees of restraint, appropriate amount of expansion to compensate the restrained tensile strain due to shrinkage in all different locations must be considered.
3. The level of expansion strain is low near the top surface of the slabs, pavements, and outer face of the east wall. These locations are highly affected by moisture

loss on the exposed concrete surfaces. However, the measurement showed expansion strains in the slabs and pavements. This verifies the effectiveness of expansive concrete to compensate restrained tensile strain due to concrete shrinkage under restrained conditions.

4. External restraint from the base friction due to a rough layer of crushed gravel plays an important role in slab on grade (pavement). The long direction of the pavements is highly affected by this type of restraint, and as a result, low expansion can be observed in the longitudinal direction of the pavement.
5. To summarize all the measurement results in reinforced concrete structures in the construction sites, the degree of restraint in each specific area affects the level of expansion, and shrinkage strains. Apart from the restrained conditions, moisture loss also plays an important role in the levels of expansion and shrinkage strains.
6. A simple prediction of restrained strains from free strains by finite element (FE) analysis shows a good agreement between the FEA and the experimental results.
7. The effectiveness of expansive concrete for compensating shrinkage (tensile) strain can also be observed from the strain distribution results obtained from FE analysis.

5.2 Recommendations for future studies

1. The strain measurement in free condition specimen should be performed using strain gauge in order to record the free strain since the concrete casting time (day 0).
2. By using previous experimental results of specimens with verification from finite element analysis, the implementation of reduction factors equations should be developed for “effective free expansion” based on free strain profiles with respect to different amount of expansive concrete and different degrees of restraint.
3. Previous measurement results from actual structures should be verified with FE analysis by using “effective free expansion” strain. Based on FE models, the numerical equations should be implemented for obtaining the relationship between the degree of restraint, stiffness, and amount of EA.

4. The levels of expansion and shrinkage due to time-dependent creep in reinforced concrete structures should be investigated and included.
5. Finally, the guideline for the design of structures using EA concrete should be proposed, to be able to calculate the required amount of EA for various degrees of restraint.



REFERENCES

- ACI Committee 223 (2010). ‘Standard Practice for the Use of Shrinkage-Compensating Concrete (ACI-223-10)’. Am. Conc. Inst., 16 p.
- Adriano, R., Sergio, T., Maurizio, M., Massimo, B., & Giovanni, A. P. (2015). Analysis of a jointless floor with calcium sulpho-aluminate and portland cement. *ACI Symposium Publication*, 305,
- ASTM C157 / C157M-08, Standard Test Method for Length Change of Hardened Hydraulic-Cement Mortar and Concrete, ASTM International, West Conshohocken, PA, 2017, www.astm.org
- ASTM C39 / C39M-08, Standard Test Method for Compressive Strength of Cylindrical Concrete Specimens, ASTM International, West Conshohocken, PA, 2018, www.astm.org
- ASTM C78 / C78M-08, Standard Test Method for Flexural Strength of Concrete (Using Simple Beam with Third-Point Loading), ASTM International, West Conshohocken, PA, 2018, www.astm.org
- ASTM C878 / C878M-08, Standard Test Method for Restrained Expansion of Shrinkage-Compensating Concrete, ASTM International, West Conshohocken, PA, 2014, www.astm.org
- Asbahan, R. E., & Vandenbossche, J. M. (2011). Effects of temperature and moisture gradients on slab deformation for jointed plain concrete pavements. *Journal of Transportation Engineering*, 137(8), 563-570. doi:10.1061/(ASCE)TE.1943-5436.0000237
- Attiyah, A., Gesund, H., Mohammed, M., Rasool, H., & Rasool, M. (2014). Finite element modelling of concrete shrinkage cracking in walls. *Kufa Journal of Engineering*, 5, 127-140.
- Carlson, R. W., & Reading, T. J. (1988). Model study of shrinkage cracking in concrete building walls. *ACI Structural Journal*, 85(4), 10.14359/2666
- Chen, C. L., Tang, C. S., & Zhao, Z. H. (2011). Application of mgo concrete in china dongfeng arch dam foundation. *Advanced Materials Research*, 168-170, 1953-1956. 10.4028/www.scientific.net/AMR.168-170.1953

- Chris Ramseyer, K. R., & Seth, R. (2016). Behavior of shrinkage compensating concrete in an unrestrained and restrained environment. *ACI Symposium Publication*, 307,
- Dung Tien Nguyen, R. S., Somnuk Tangtermsirikul. (2010). Prediction of net expansion of expansive concrete under restraint. *Engineering Journal of Research and Development*, Vol. 21 No. 3,
- Gorst, N. J. S., Williamson, S. J., Pallet, P. F., & Clark, L. A. (2003). *Friction in temporary works*, The University of Birmingham.
- Huang, K., Deng, M., Mo, L., & Wang, Y. (2013). Early age stability of concrete pavement by using hybrid fiber together with mgo expansion agent in high altitude locality. *Construction and Building Materials*, 48, 685-690. <https://doi.org/10.1016/j.conbuildmat.2013.07.089>
- Huang, K., Shi, X., Zollinger, D., Mirsayar, M., Wang, A., & Mo, L. (2019). Use of mgo expansion agent to compensate concrete shrinkage in jointed reinforced concrete pavement under high-altitude environmental conditions. *Construction and Building Materials*, 202, 528-536. <https://doi.org/10.1016/j.conbuildmat.2019.01.041>
- Ishida, T., Pen, K., Tanaka, Y., Kashimura, K., & Iwaki, I. (2018). Numerical simulation of early age cracking of reinforced concrete bridge decks with a full-3d multiscale and multi-chemo-physical integrated analysis. *Applied Sciences*, 8(3), 10.3390/app8030394
- Kanciruk, A. (2018). Long-term study of the impact of temperature changes, material aging and service load on the strains of a reinforced concrete structure. *E3S Web of Conferences*, 66, 02006. 10.1051/e3sconf/20186602006
- Kheder, G. F. (1997). A new look at the control of volume change cracking of base restrained concrete walls. *ACI Structural Journal*, 94(3), 10.14359/478
- Lam, N., Sahamitmongkol, R., & Tangtermsirikul, S. (2008). Expansion and compressive strength of concrete with expansive additive. *Research and Development Journal*, 19 (2), 40-49.
- Lam, N., Sumranwanich, T., Krammart, P., Yodmalai, D., Sahamitmongkol, R., & Tangtermsirikul, S. (2008). Durability properties of concrete with expansive additive. *Research and Development Journal*, 19 (4), 8-15.

- Li, H., Tian, Q., Zhao, H., Lu, A., & Liu, J. (2018). Temperature sensitivity of mgo expansive agent and its application in temperature crack mitigation in shiplock mass concrete. *Construction and Building Materials*, *170*, 613-618. <https://doi.org/10.1016/j.conbuildmat.2018.02.184>
- Liu, F., Shen, S.-L., Hou, D.-W., Arulrajah, A., & Horpibulsuk, S. (2016). Enhancing behavior of large volume underground concrete structure using expansive agents. *Construction and Building Materials*, *114*, 49-55. <https://doi.org/10.1016/j.conbuildmat.2016.03.075>
- Michael D. Brown, C. A. S. J. G. S. K. J. F., & John, E. B. (2007). Use of alternative materials to reduce shrinkage cracking in bridge decks. *ACI Materials Journal*, *104*(6), 10.14359/18967
- Mo, L., Deng, M., Tang, M., & Al-Tabbaa, A. (2014). Mgo expansive cement and concrete in china: Past, present and future. *Cement and Concrete Research*, *57*, 1-12. <https://doi.org/10.1016/j.cemconres.2013.12.007>
- Neville, A. M., & Brooks, J. J. (2010). *Concrete technology*. Pearson Education Limited, Edinburgh Gate, Harlow, Essex CM20 2JE, England: Longman Group UK Limited
- Newell, S., & Goggins, J. (2017). Real-time monitoring of concrete–lattice-girder slabs during construction. *Proceedings of the Institution of Civil Engineers - Structures and Buildings*, *170*, 885-900. 10.1680/jstbu.16.00198
- Newell, S., & Goggins, J. (2018). Investigation of thermal behaviour of a hybrid precast concrete floor using embedded sensors. *International Journal of Concrete Structures and Materials*, *12*(1), 10.1186/s40069-018-0287-y
- Nguyen, D., Sahamitmongkol, R., Lam, N., Tongaroonsri, S., & Tangtermsirikul, S. (2010). Prediction of shrinkage cracking age of concrete with and without expansive additive. *Songklanakarinn Journal of Science and Technology*, *32*,
- Nguyen, T. B. T., Chatchawan, R., Saengsoy, W., Tangtermsirikul, S., & Sugiyama, T. (2019). Influences of different types of fly ash and confinement on performances of expansive mortars and concretes. *Construction and Building Materials*, *209*, 176-186. <https://doi.org/10.1016/j.conbuildmat.2019.03.032>

- Pakorn Sutthiwaree, R. S., Somnuk Tangtermsirikul. (2015). Effect of internal curing on expansion and shrinkage of expansive concrete. *Science & Technology Asia (STA)*, Vol.20 No.4,
- RawiI, R. S. A., & Kheder, G. F. (1990). Control of cracking due to volume change in base-restrained concrete members. *ACI Structural Journal*, 87(4), 10.14359/2747
- Rebibou, S. J., Dux, P. F., & Nooru-Mohamed, M. B. (2003). Shrinkage in concrete pavements. *Australian Journal of Civil Engineering*, 1(1), 23-28. 10.1080/14488353.2003.11463908
- Richardson, J., Schiller, S. E. B., & Mike, J. (2010). Measured strains in post-tensioned concrete parking deck made with shrinkage-compensating concrete. *ACI Structural Journal*, 107(6), 10.14359/51664020
- Schwer, L. E., & Malvar, L. J. (2005). Simplified concrete modelling with *mat_concrete_damage_rel3. *JRI LS-DYNA USER WEEK*,
- Seongcheol, C., & Moon, C. W. (2010). Thermal strain and drying shrinkage of concrete structures in the field. *ACI Materials Journal*, 107(5), 10.14359/51663970
- Tongaroonsri, S., & Tangtermsirikul, S. (2008). Influence of mixture condition and moisture on tensile strain capacity of concrete. *ScienceAsia*, 34, 59-68. 10.2306/scienceasia1513-1874.2008.34.059
- Wee, T., Swaddiwudhipong, S., & Lu, H. (2000). Tensile strain capacity of concrete under various states of stress. *Magazine of Concrete Research - MAG CONCR RES*, 52, 185-193. 10.1680/macr.2000.52.3.185
- William, G. W., Shoukry, S. N., & Riad, M. Y. (2005). Early age cracking of reinforced concrete bridge decks. *Bridge Structures*, 1(4), 379-396. 10.1080/15732480500483828
- Wu, Y., Crawford, J. E., & Magallanes, J. M. (2012). Performance of ls-dyna concrete constitutive models. In (Ed.), *12th International LS-DYNA Users Conference*
- Yu, L., Deng, M., Mo, L., Liu, J., & Jiang, F. (2019). Effects of lightly burnt mgo expansive agent on the deformation and microstructure of reinforced concrete wall. *Advances in Materials Science and Engineering*, 2019, 1-9. 10.1155/2019/1948123



APPENDIX

APPENDIX A

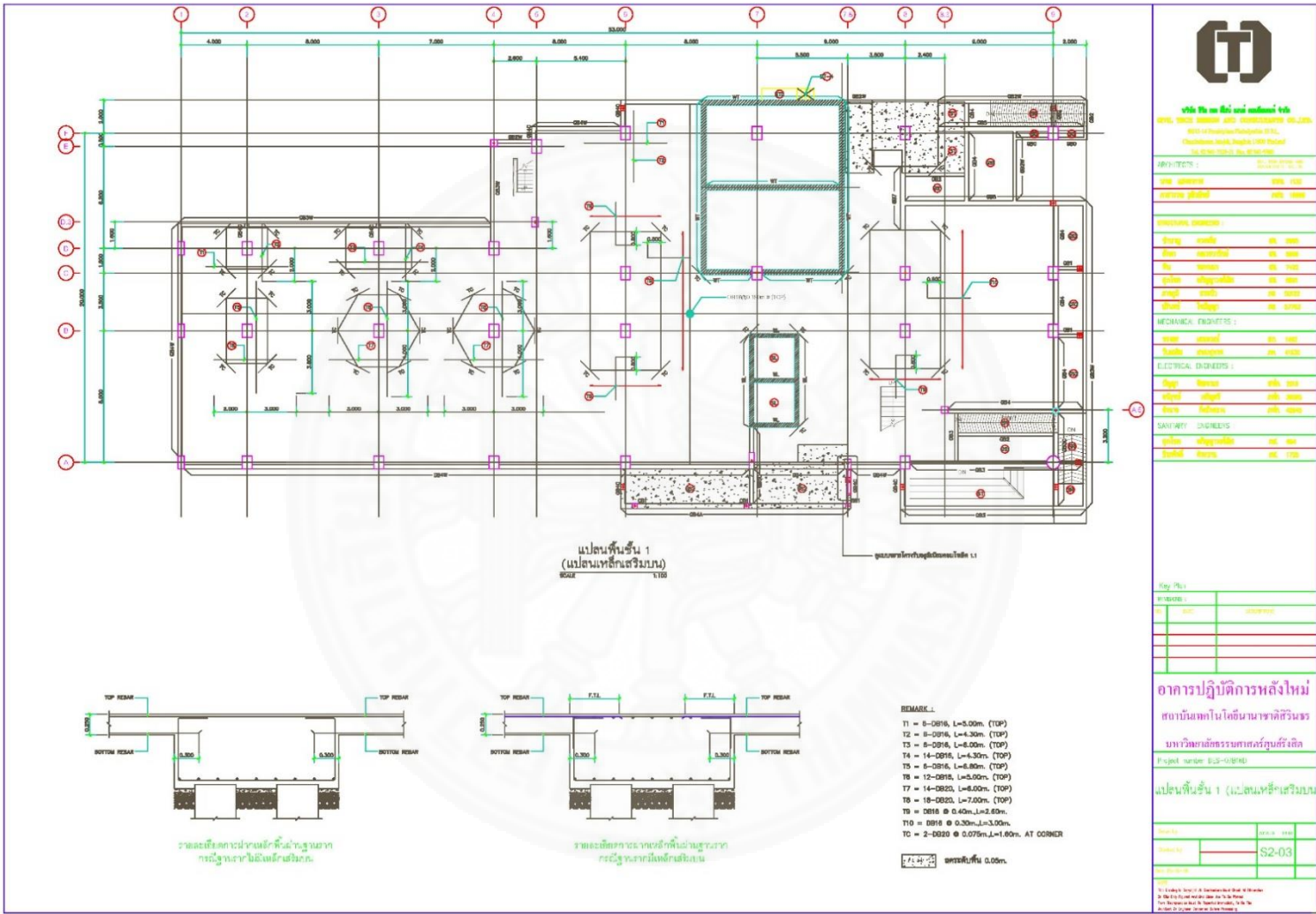


Figure A 1 Reinforcement layout drawing of top steel on beam and foundation

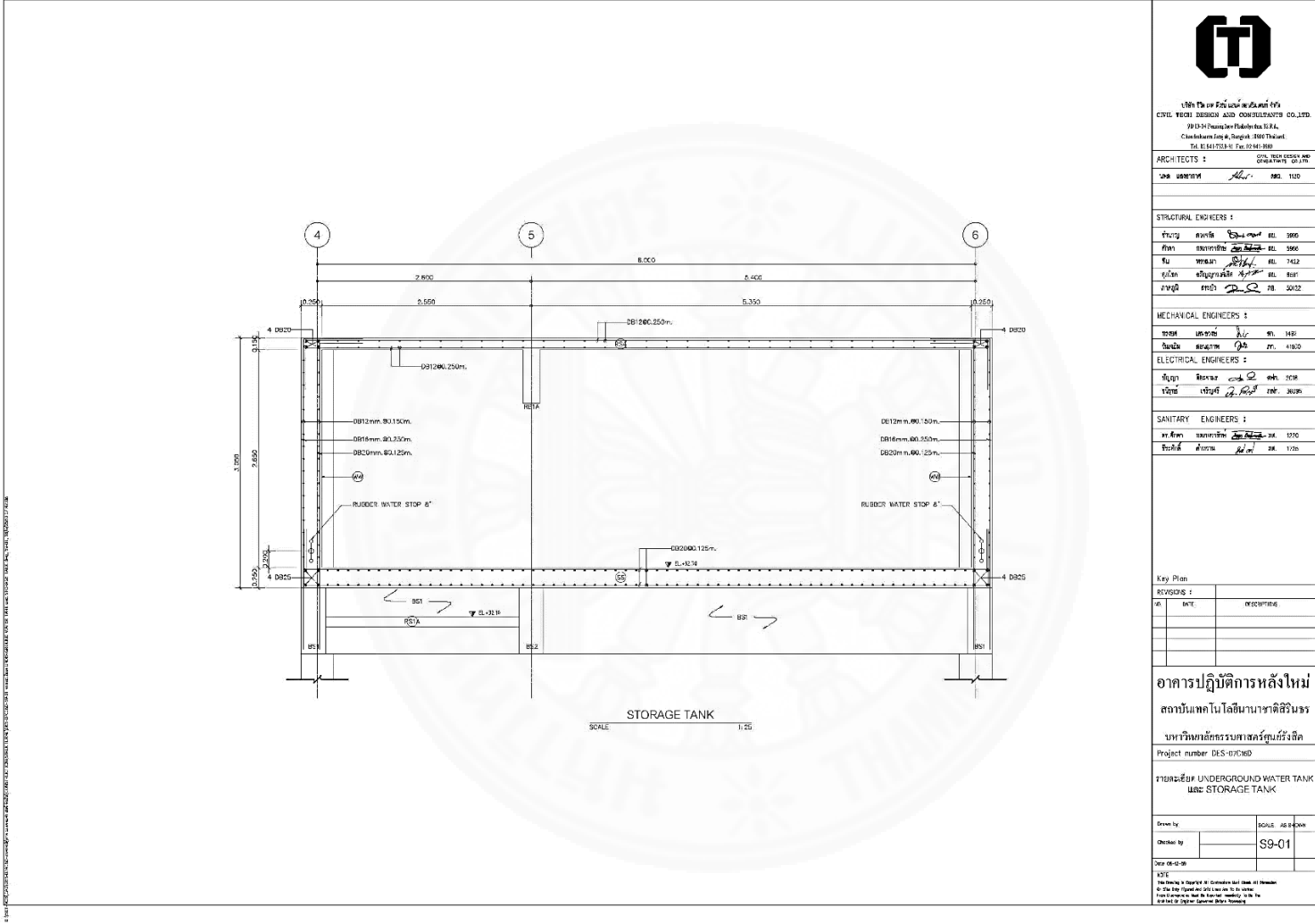


Figure A 3 Typical section of water tank walls for both section A-A and section B-B

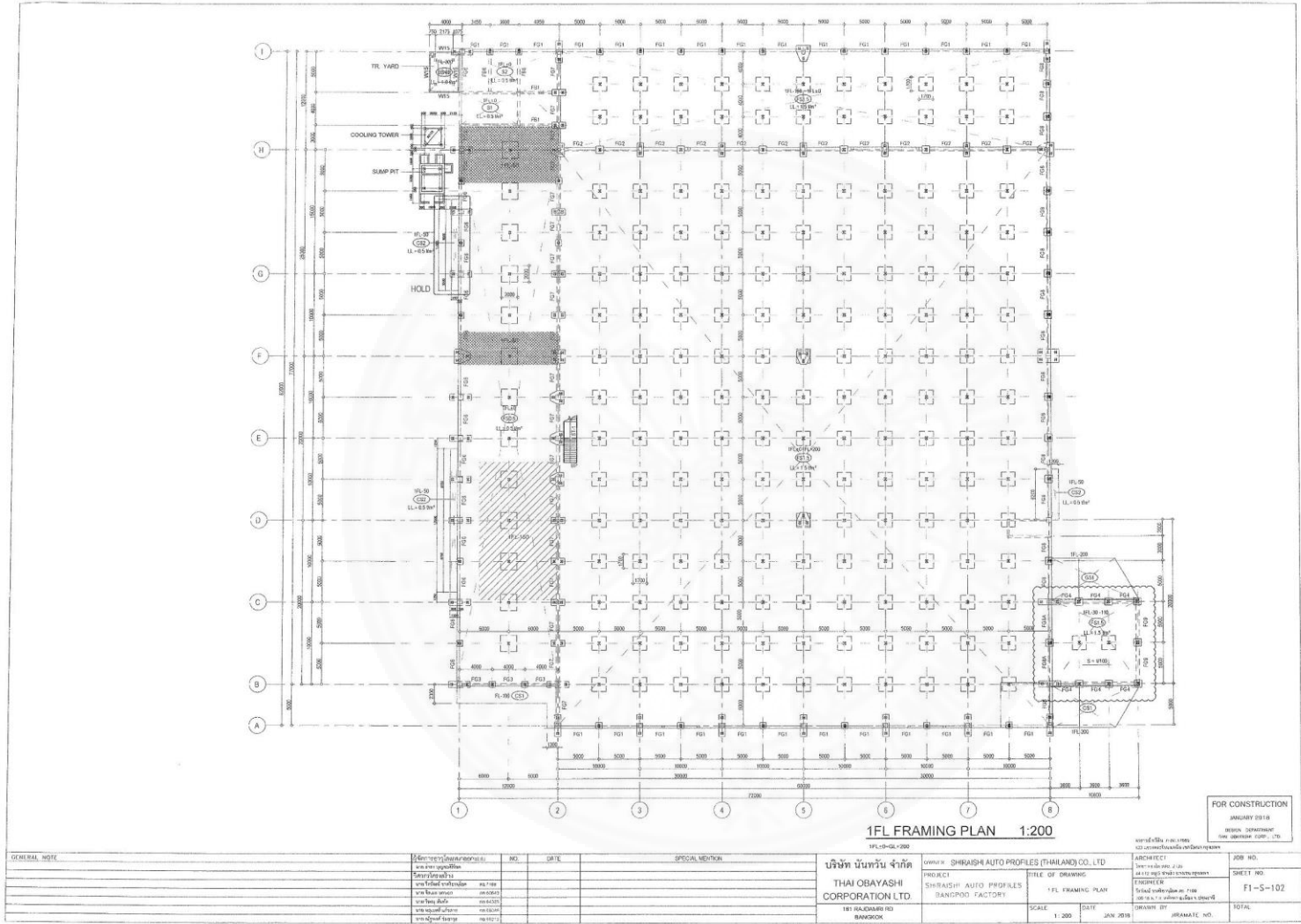


Figure A 5 First floor framing plan of industrial slab

BEAM LIST 1:30																								
SYMBOL	FG1			FG2			FG3			FG4			FG5			FG7			FG8					
	EXT. END	CENT.	INT. END	EXT. END	CENT.	INT. END	EXT. END	CENT.	INT. END	EXT. END	CENT.	INT. END	EXT. END	CENT.	INT. END	EXT. END	CENT.	INT. END	EXT. END	CENT.	INT. END			
SECTION																								
UPPER BAR	4-020	2-020	4-020	4-025	4-025	6-025	2-020	2-020	4-020	4-020	2-020	6-020	3-020	2-020	5-020	4-025	4-025	6-025	4-020	2-020	6-020			
LOWER BAR	4-020	4-020	2-020	4-025	6-025	4-025	3-020	4-020	2-020	4-020	6-020	2-020	3-020	3-020	2-020	4-025	6-025	4-025	4-020	6-020	2-020			
STIRRUP	D10@100	D10@150	D10@100	D10@150 (2 Laps)	D10@150	D10@150 (2 Laps)	D10@200	D10@100	D10@150	D10@150	D10@100	D10@150	D10@150	D10@150	D10@150	D10@150 (2 Laps)	D10@150	D10@150 (2 Laps)	D10@100	D10@150	D10@100			
WEB BAR	2-D10L/PH900 AT CENTER			2-D10L/PH900 AT CENTER			2-D10L/PH900 AT CENTER			2-D10L/PH900 AT CENTER			2-D10L/PH900 AT CENTER			2-D10L/PH900 AT CENTER			2-D10L/PH900 AT CENTER					
SYMBOL	FG9			FG10			FG11			FG12			FG13			FG14			FG15					
POSITION	CENT.			EXT. END			CENT.			EXT. END			CENT.			EXT. END			CENT.					
SECTION																								
UPPER BAR	4-020	4-020	2-020	3-020	3-020	5-020	2-025	2-025	2-025	2-025	2-025	2-025	2-025	2-025	2-025	2-025	2-025	2-025	2-025	2-025	2-025			
LOWER BAR	4-020	4-020	2-020	3-020	3-020	5-020	2-025	2-025	2-025	2-025	2-025	2-025	2-025	2-025	2-025	2-025	2-025	2-025	2-025	2-025	2-025			
STIRRUP	D10@150	D10@150	D10@150	D10@150	D10@150	D10@150	D10@150	D10@150	D10@150	D10@150	D10@150	D10@150	D10@150	D10@150	D10@150	D10@150	D10@150	D10@150	D10@150	D10@150	D10@150			
WEB BAR	2-D10L/PH900 AT CENTER			2-D10L/PH900 AT CENTER			2-D10L/PH900 AT CENTER			2-D10L/PH900 AT CENTER			2-D10L/PH900 AT CENTER			2-D10L/PH900 AT CENTER			2-D10L/PH900 AT CENTER					
SYMBOL	Z01		Z02		Z03		Z04		Z05		Z06		Z07		Z08		Z09		Z10		Z11			
POSITION	CENT.		EXT. END		ALL		CENT.		EXT. END		CENT.		EXT. END		CENT.		EXT. END		CENT.		EXT. END			
SECTION																								
UPPER BAR	7-025	7-025	3-025	11-025	11-025	3-020	2-020	4-020	2-020	2-020	4-020	2-020	2-020	4-020	2-020	2-020	4-020	2-020	2-020	4-020	4-020			
LOWER BAR	14-025	11-025	3-020	21-025	18-025	3-020	3-020	2-020	3-020	3-020	2-020	3-020	3-020	2-020	3-020	3-020	2-020	3-020	3-020	3-020	3-020			
STIRRUP	D10@150	D10@150	PH900	D10@150	D10@150 (2 Laps)	PH900	PH900	PH900	PH900	PH900	PH900	PH900	PH900	PH900	PH900	PH900	PH900	PH900	PH900	PH900	PH900			
WEB BAR	2-D10L/PH900 AT CENTER		2-D10L/PH900 AT CENTER		2-D10L/PH900 AT CENTER		2-D10L/PH900 AT CENTER		2-D10L/PH900 AT CENTER		2-D10L/PH900 AT CENTER		2-D10L/PH900 AT CENTER		2-D10L/PH900 AT CENTER		2-D10L/PH900 AT CENTER		2-D10L/PH900 AT CENTER		2-D10L/PH900 AT CENTER			
SYMBOL	LB1		Z01		Z02		Z03		Z04		Z05		Z06		Z07		Z08		Z09		Z10			
POSITION	ALL		EXT. END & CENT.		INT. END		ALL		EXT. END		CENT.		EXT. END		CENT.		EXT. END		CENT.		EXT. END			
SECTION																								
UPPER BAR	2-025	2-025	2-025	4-025	4-025	2-025	2-025	2-025	2-025	2-025	2-025	2-025	2-025	2-025	2-025	2-025	2-025	2-025	2-025	2-025	2-025			
LOWER BAR	4-025	4-025	4-025	2-025	2-025	2-025	2-025	2-025	2-025	2-025	2-025	2-025	2-025	2-025	2-025	2-025	2-025	2-025	2-025	2-025	2-025			
STIRRUP	PH900	PH900	PH900	PH900	PH900	PH900	PH900	PH900	PH900	PH900	PH900	PH900	PH900	PH900	PH900	PH900	PH900	PH900	PH900	PH900	PH900			
WEB BAR	2-D10L/PH900 AT CENTER		2-D10L/PH900 AT CENTER		2-D10L/PH900 AT CENTER		2-D10L/PH900 AT CENTER		2-D10L/PH900 AT CENTER		2-D10L/PH900 AT CENTER		2-D10L/PH900 AT CENTER		2-D10L/PH900 AT CENTER		2-D10L/PH900 AT CENTER		2-D10L/PH900 AT CENTER		2-D10L/PH900 AT CENTER			

Figure A 6 Beam lists of industrial floor slab

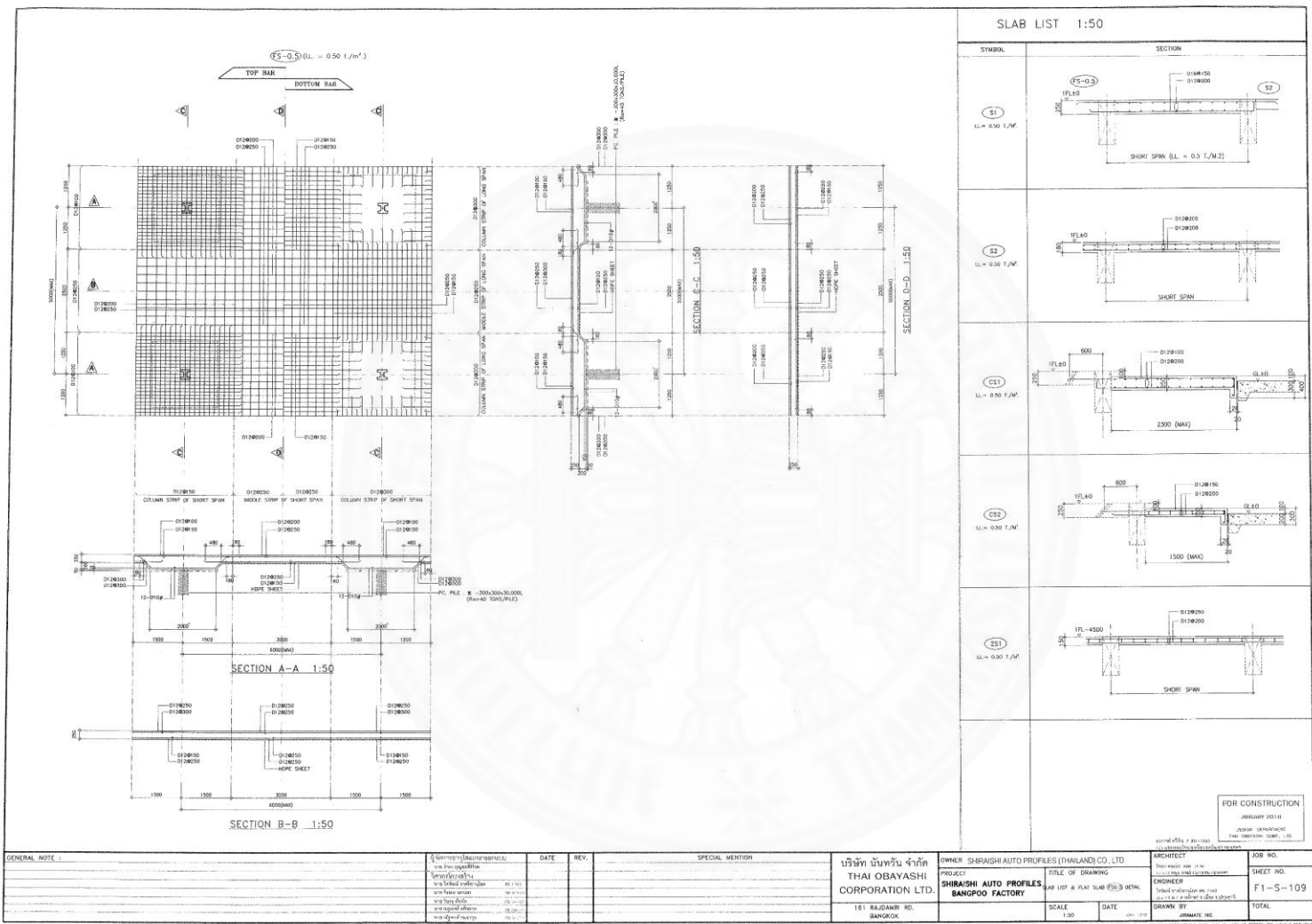


Figure A 7 Reinforcement layout of industrial floor slab for live load = 0.5 ton/m²

BIOGRAPHY

Name	Ms. Su Hlaing Myint
Date of Birth	August 18, 1992
Education	2013 :Bachelor of Engineering (Civil Engineering) Technological University (Mandalay), Myanmar 2017 :Master of Engineering (Civil, Structure) Yangon Technological University, Myanmar
Publications	

